Self-Archived version:
Javier Luque Di Salvo, Alessandro Cosenza, Andrea Cipollina, Alessandro Tamburini, Giorgio Micale.
Long-run operation of a Reverse Electrodialysis system fed with wastewaters. *Journal of Environmental Management*, 217 (2018) 871-887. https://doi.org/10.1016/j.jenvman.2018.03.110

Long-run operation of a Reverse Electrodialysis system fed with wastewaters

Javier Luque Di Salvo[a], Alessandro Cosenza[a], Alessandro Tamburini[a]*, Giorgio Micale[a], Andrea Cipollina[a]

[a]*Dipartimento dell'Innovazione Industriale e Digitale - Ingegneria Chimica, Gestionale, Informatica, Meccanica (DIID), Università di Palermo (UNIPA) – viale delle Scienze Ed.6, 90128 Palermo, Italy.*

*e-mail: alessandro.tamburini@unipa.it

Abstract

The performance of a Reverse ElectroDialysis (RED) system fed by unconventional wastewater solutions for long operational periods is analysed for the first time. The experimental campaign was divided in a series of five independent long-runs which combined real wastewater solutions with artificial solutions for at least 10 days. The time evolution of electrical variables, gross power output and net power output, considering also pumping losses, was monitored: power density values obtained during the long-runs are comparable to those found in literature with artificial feed solutions of similar salinity. The increase in pressure drops and the development of membrane fouling were the main detrimental factors of system performance. Pressure drops increase was related to the physical obstruction of the feed channels defined by the spacers, while membrane fouling was related to the adsorption of foulants over the membrane surfaces. In order to manage channels partial clogging and fouling, different kinds of easily implemented *in situ* backwashings (i.e. neutral, acid, alkaline) were adopted, without the need for an abrupt interruption of the RED unit operation. The application of periodic ElectroDialysis (ED) pulses is also tested as fouling prevention strategy. The results collected suggest that RED can be used to produce electric power by unworthy wastewaters, but additional studies are still needed to characterize better membrane fouling and further improve system performance with these solutions.

Keywords: salinity gradient power; reverse electrodialysis; ion exchange membranes; fouling; fish wastewater; reclaimed water.

1. INTRODUCTION

Salinity Gradient Power (SGP) is an attractive alternative to produce renewable energy without any environmental issue and with a high potential of power production worldwide (Alvarez-Silva et al., 2016; Daniilidis et al., 2014; Tedesco et al., 2015a; Veerman et al., 2009). It is based on the simple concept of mixing two waters of different salinity and collecting the free energy that is spontaneously produced during this process. If the mixing process is properly controlled, net energy can be extracted.

There are several technologies designed to control water mixing in different stages of development (Jia et al., 2014), among which Pressure Retarded Osmosis (PRO) (Helfer et al., 2014; Sarp et al., 2016), Reverse ElectroDialysis (RED) (Yip et al., 2014) and Accumulator mixing techniques (Capacitive mixing –CapMix (Rica et al., 2013), and Mixing Entropy Battery –MEB (La Mantia et al., 2011)) deserve mention. Some of these techniques have already been considered for practical applications in site-specific analysis (Emdadi et al., 2016; Helfer and Lemckert, 2015; Tedesco et al., 2017, 2016). In particular, of all current SGP techniques, RED has experienced a sharp growth in terms of understanding and optimization in the last years (Güler et al., 2014; Gurreri et al., 2012; La Cerva et al., 2017; Straub et al., 2016), with the advantage that is able to deal with very high salinity solutions, a challenge that is found in PRO (Schaetzle and Buisman, 2015).

An interesting feature of the RED technology is its flexibility in the feed possibilities available to use. Most studies are devoted to artificial salt solutions (Bevacqua et al., 2017, 2016; Daniilidis et al., 2014b; M. Tedesco et al., 2015b), some to real waters (D'Angelo et al., 2017; Tedesco et al., 2016; Veerman et al., 2009), while very few studies are devoted to the exploitation via RED of the salinity gradient available in wastewater solutions. This exploitation can give value to an otherwise discard product and can additionally increase the quantity of sources suitable for salinity gradient power technologies.

In this sense, several industrial processes require high amounts of salt, generating effluents with high salinity levels, similar to those found in seawater, or even higher, as the case of fish processing, textile dyeing, petroleum derivatives and tanneries (Lefebvre and Moletta, 2006; Sivaprakasam et al., 2008; Xiao and Roberts, 2010). One of the issues to solve for these kind of wastewaters is the high-salinity of the effluents, which needs to be diluted before discard to minimize environmental impact (Cambridge et al., 2017; Roberts et al., 2010), a process that can be accomplished (at least partially) by RED technology. On the other hand, low salinity effluents are more readily available, like those coming from urban waste disposals (Raffin et al., 2013). This opens a wide spectrum of new feed sources for salinity gradient power still to be explored.

To the date there are not much studies dealing with wastewater re-use to produce energy from

SGP technologies. D'Angelo et. al. demonstrated the possibility of using RED in wastewater treatment by successfully removing Acid orange 7, while operating the first RED pilot plant fed with real brine and brackish water in a long duration experimental campaign (D'Angelo et al., 2017). Wang et. al. used a phenol-containing wastewater to feed a RED unit with the objective of recovering phenol derivatives, proving the possibility of coupling RED with ED in the wastewater treatment process (Wang et al., 2017). Very recently, Kingsbury et. al. studied the response of a RED unit fed with five different pairs of real waters and wastewaters and remarked the role of organic fouling in the severe detriment of power density (Kingsbury et al., 2017). However, to the authors' knowledge there are still no studies in literature related to the long-term effects that these kinds of feeds may produce on the overall RED unit performance and on the possible strategies to prevent or reverse their potential damage. Thus, in order to understand whether RED is capable to benefit from these otherwise unworthy wastewaters, we performed long duration experiments and evaluated the system time-evolution. The so-called long-runs can also give light into the feasibility of an enduring energy production via a RED unit continuously fed by wastewaters for a realistic period of operational time. In particular, wastewater originated in a fish canning factory, and wastewater coming from urban water disposal, were used as high and low salinity feeds, respectively (Figure 1).

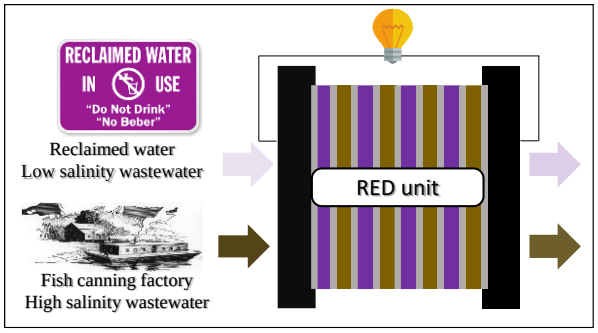

Figure 1. Flow chart showing wastewater effluents feeding a RED unit and generating a power output. The salinity of feeds exiting the stack changes during the process: fish wastewater dilutes while reclaimed water concentrates.

When using feeds from wastewater treatment plants, the time-dependent behaviour of ion exchange membranes in long-run operations is subjected to fouling phenomena (Kingsbury et al., 2017; Vaselbehagh et al., 2017; Vermaas et al., 2013). Fouling mechanisms consist in the attachment, adsorption and accumulation of pollutants over the surface or inside the membrane, leading to an alteration of the membrane material and/or to pores obstruction that hinders transport of permeates thus reducing the process performance (Guo et al., 2012).

The anti-fouling techniques to be applied will depend on the type of fouling that is produced, which can be classified as inorganic (scaling), organic or colloidal fouling, and biofouling (Mikhaylin and Bazinet, 2016). In the case of (Reverse) ElectroDialysis systems, AEMs are mainly affected by organic fouling (Lee et al., 2009) and/or biofouling (Vaselbehagh et al., 2017), while

scaling by inorganic species (Ca^{2+}, Mg^{2+}) can be quite common on CEMs (Mikhaylin and Bazinet, 2016; Vermaas et al., 2013). An easy and suitable strategy to prevent and control fouling in RED systems consists in periodic (back) washing techniques with deionized water and/or chemical cleaning agents (Garcia-Vasquez et al., 2016; Mikhaylin and Bazinet, 2016). In particular, alkaline solutions should be more effective in order to treat organic fouling, while the use of acid reagents should be more effective in removing scaling produced by inorganic species.

It is worth to mention that besides fouling, clogging of channels may also occur, especially if the channels are thin and filled with meshed-spacers. The obstruction is physical rather than physical-chemical like the stronger interactions established in fouling processes, so if the backwashing is proven effective in reversing fouling is expected to also unclog the spacer-filled channels. Channel clogging can be very important in RED as it can also contribute to an increase of pressure drops and thus affect the net power density generated (Gurreri et al., 2016, 2012; La Cerva et al., 2017).

The objective of this work is that of analysing for the first time the performance during long-run tests of a RED unit operated with real feed solutions of different origin and salinity, but both coming from a biological wastewater treatment plant. As a first step, system was operated with artificial solutions to determine the best operating conditions and then, switching to real wastewater solutions, the behaviour of the RED process was analysed during long-run tests. Five independent long-runs were performed, the first three devoted to system characterization, while the last two mainly devoted to system performance improvement.

To the best of our knowledge, this is the first attempt in the literature to investigate a RED system fed with real wastewater solutions running uninterruptedly for such a long period.

2. EXPERIMENTAL SECTION

2.1 Experimental Setup

The RED unit investigated consisted of 10 piled cell-pairs with an active membrane area of 10x10 cm^2. A cell-pair consisted of a dilute channel (Low), an Anion Exchange Membrane (AEM), a concentrate channel (High) and a Cation Exchange Membrane (CEM). Polyamide woven spacers 270 μm thick (Deukum GmbH, Germany) between membranes were used as feed channels. Woven spacers were preferred to profiled membranes because different possible clogging issues in the dilute and concentrate channels (due to a different wastewater solution) may result into a differential pressure between the two channels. When the channel dimensional stability is not guaranteed by a spacer, membranes can be significantly deformed thus changing the open area of the two channels, in the worst case leading to the complete occlusion of the channel and to the stop of the long-run.

Ion Exchange Membranes (IEMs) were kindly supplied from FUJIFILM Manufacturing Europe BV (CEM Type I and AEM Type I), whereas Nafion® CEM were used to separate the cell-pairs stack from electrode compartments. Two Ru-Ir oxide-coated Ti electrodes (Magneto Special Anodes BV) were placed in both end compartments. Before mounting the RED unit, a standard pre-treatment procedure was adopted to prepare membranes, keeping IEMs in a solution of NaCl 0.5 M for 24 hours.

Real, treated wastewater samples were specially handled and stored before being used as feeds (see Section 2.2). Ion chromatography analysis was employed to quantify cations and anions composition in wastewaters (IC 822 Compact Plus Metrohm, Metrosep C4-250/4.0 and Metrosep ASupp5-250/4.0). Artificial feed solutions were prepared with high grade ultra-pure sodium chloride (NaCl 99.8% Sigma Aldrich) and demineralized water.

The Electrode Rinse Solution (ERS) was constituted of 0.100 M $K_3[Fe(CN)_6]$ (Sigma Aldrich), 0.100 M $K_4[Fe(CN)_6]\cdot 3H_2O$ (Sigma Aldrich) and 0.050 M of ultra-pure sodium chloride (NaCl 99.8% Sigma Aldrich) as supporting electrolyte (0.300 M NaCl for long-run V), giving a final ERS salt molarity of 0.250 M (0.500 M for long-run V). Acid and alkaline solutions for cleaning procedures were prepared with hydrochloric acid (HCl 37% Sigma Aldrich) and sodium hydroxide (solid NaOH > 99%, Sigma Aldrich), respectively. Standard grade hypochlorite was used once for a cleaning procedure.

The test rig for the experimental campaign is sketched in Figure 2. Two peristaltic pumps (Cellai, mod. 503U) were used to feed the solutions into the stack at the desired velocities, with a co-current arrangement, entering the bottom and exiting at the top of the RED unit. Pressure gauges (M 40 PA, Cewal) and thermocouples with relevant data logger (Thermometer YC-747D, YCT) were placed at the inlet of each channel to monitor pressure and temperature of feed solutions. A smaller peristaltic pump (Verderflex R2S) was used to recirculate the Electrode Rinse Solution. The glass tank containing the ERS and the pipes connecting it to the RED unit were well sealed and covered with aluminium paper to avoid contact with air and exposure to light, to prevent degradation (Scialdone et al., 2013).

In order to characterize the RED unit electrical performance, a manual switch containing external calibrated resistors was connected in series with the RED unit as external load, and the voltage drop for each value of external resistance was measured (Multimeter Digimaster DM58B) and post-processed.

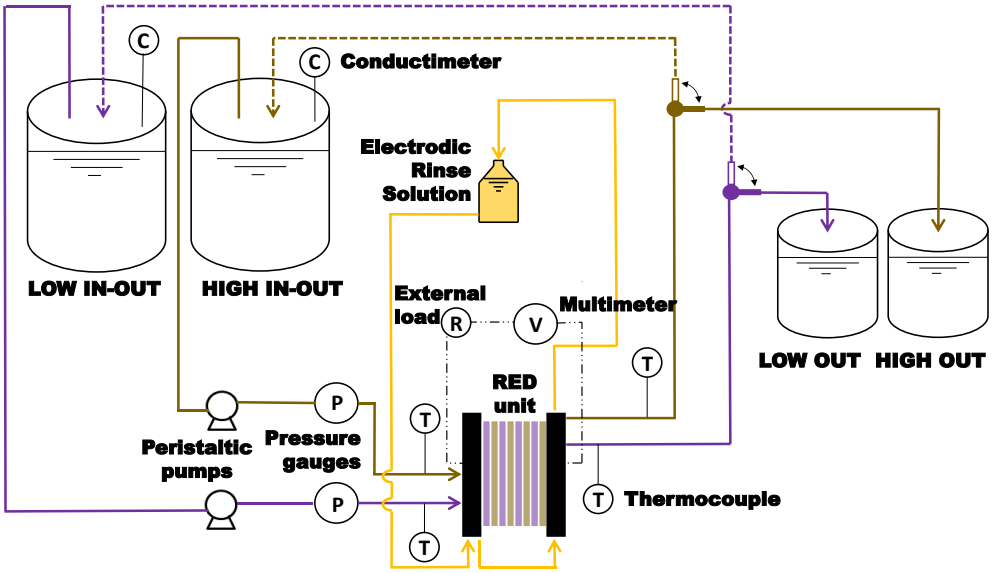

Figure 2. Schematic diagram of experimental setup showing the two operating modes: once-through mode (straight line) and recirculating mode (dashed lined).

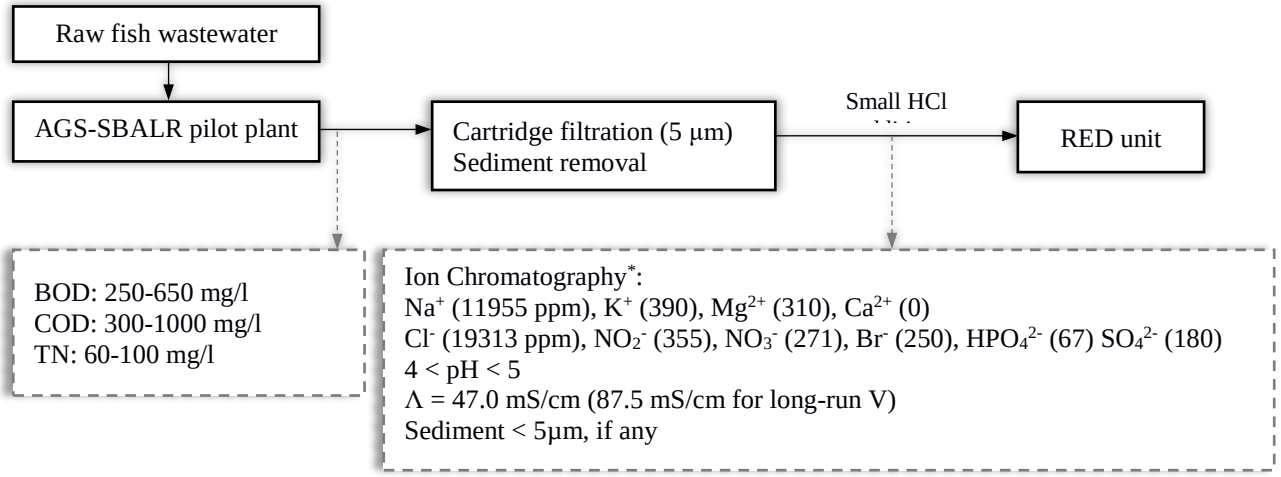

Figure 3. Diagram showing treatments and physical-chemical characteristics of fish wastewater before feeding the RED unit. The AGS-SBALR module can operate up to a salinity of 75 g/l.

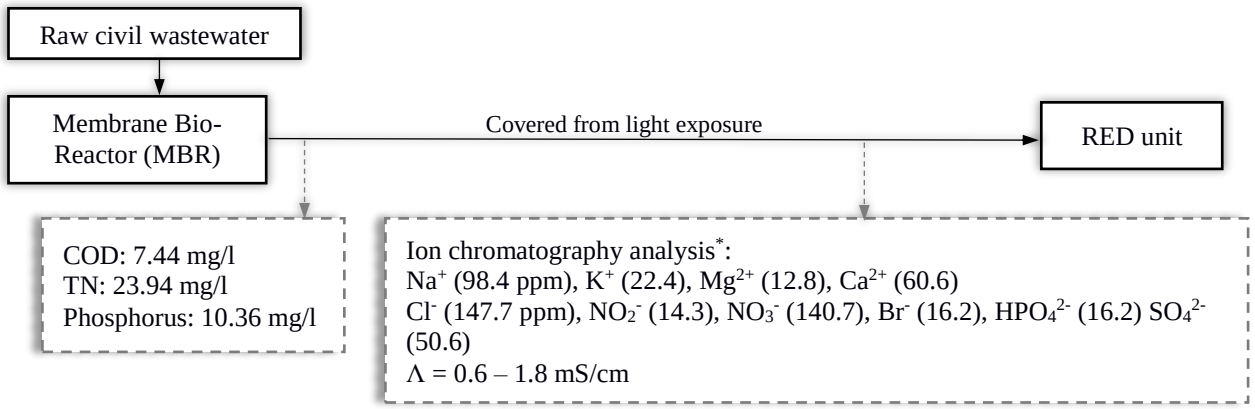

Figure 4. Diagram showing treatments, physical-chemical characteristics and storage conditions of civil wastewater before feeding the RED unit. *Values obtained by Ion Chromatography: these values may variate with respect to the samples used in the long-runs, which depend on the properties of day-by-day raw civil wastewater inlet entering the MBR.

2.2 Properties of feed solutions

2.2.1 High concentration wastewater

The high concentration wastewater originates from a local fish canning factory located at Aspra (Palermo, Italy). Fish processing requires large amounts of water and salt to guarantee cleaning and sanitation of the final product. In general, fish industry effluents are characterized by high concentration of suspended solids, organic matter, nitrogen derivatives and salt, mainly sodium chloride. Biological treatments are typically conditioned by the high salinity, making the use of common non-halophilic bacteria unsuitable. In this sense, the use of an active Aerobic Granular Sludge (AGS) has proven to be effective for treating this kind of wastewater (Capodici et al., 2018; Corsino et al., 2016; Wang et al., 2015).

In particular, in the present case, the high salinity effluent was preliminarily treated in a pilot AGS Sequence Batch Air-Lift Reactor (SBALR) system for organic carbon abatement, with a simultaneous nitrification – denitrification procedure, at the Department of Civil, Environmental and Materials Engineering (DICAM) of the University of Palermo (Italy), through an innovative technique for high salinity wastewater (Corsino et al., 2016). This process shows 90% of efficiency in Total Organic Carbon (TOC) removal regardless of the level of salinity of the water (up to 75 g/l).

All of the fish wastewater samples coming from the AGS pilot plant were further filtrated with standard cartridge filters (size of 5 μm) to remove remaining suspended solids (if any) that could be present after the sedimentation step. Moreover, a small amount of HCl was added to maintain $4 < pH < 5$ in order to disfavour bacteria growth without compromising IEMs material.

2.2.2 Low concentration wastewater

Reclaimed water from urban Waste-Water Treatment (WWT) plant was used as the low concentration feed solution. The use of such type of feed solution opens room for a significant exploitation potential in RED technology. In fact, wastewater treatment technologies are well developed and plants are operating in most populated areas of the world. In addition to that, the recent implementation of technologies based on the use of Membrane BioReactors (MBR) would allow an even larger potential due to the extremely improved quality of the treated effluent leaving the WWT plant (Hirani et al., 2013; Raffin et al., 2013).

In particular, the wastewater used in this work was treated in an experimental MBR pilot plant (capacity: 6 lt/h) that follows the classical University of Cape Town (UCT) scheme (Cosenza et al., 2013), in which the settler is replaced with a compartment containing two membrane modules in a side-stream configuration. Also this plant is located at the premises of the Department of Civil, Environmental and Materials Engineering (DICAM) of the University of Palermo.

The treated effluent is a low turbidity reclaimed water with an electric conductivity (Λ) within the range 0.6 – 1.8 mS/cm. No further treatment for the samples was required, which represents an advantage of MBR compared to conventional WWT plant. The only requirement was the storage in dark, covered tanks to reduce algae proliferation due to nutrients availability in the reclaimed water.

Figure 4 reports the main physical-chemical properties of the low concentration effluent used for RED operations.

2.2.3 Artificial solutions

Artificial solutions were adopted to simulate the salinity of wastewater solutions. They were prepared from deionized water and sodium chloride. The concentrations of the artificial solutions were chosen in order to mimic the electrical conductivity of the real samples, meaning that ions other than Na^+ and Cl^- were not considered.

2.3 Experimental procedure

Experiments were performed following the standard experimental procedures presented in the literature for RED laboratory units testing (Bevacqua et al., 2016; Veerman et al., 2010). The RED unit was fed with the high salinity and low salinity solutions and electrical variables were measured while varying the external load and so calculating all figures of merit typical of a RED system. In particular, the Open Circuit Voltage (OCV_{exp}), the stack voltage (E_{stack}) and the stack current (I_{stack}) were measured and their value was used to infer the other variables. The stack electrical resistance (R_{stack}) was determined from the slope of the linear response of E_{stack} *vs.* I_{stack}. Likewise, the gross power density ($P_{d,gross}$) curve was obtained by normalizing for the number of cell pairs (N) and the active cell-pair area (A). The maximum of the $P_{d,gross}$ *vs* E_{stack} curve corresponds to the condition where R_{stack} equals the external load resistance. All results refer to this condition. Furthermore, the apparent average perm-selectivity of a couple of IEMs (AEM and CEM), named α_{app}, can be estimated by the ratio of the measured OCV_{exp} and the theoretical OCV (OCV_{ideal}) calculated from the Nernst equation. A typical correction when considering scale-up consist in subtracting the blank resistance (R_{blank}) (Bevacqua et al., 2016) to R_{stack}. R_{blank} accounts for the electrical resistance of the ERS solution and one of the end membranes and can be reasonably neglected when a large number of cell-pairs is used. Subtraction of R_{blank} gives the so-called corrected power density ($P_{d,corr}$). Finally, the energy consumption due to pumping the feed solutions into the RED unit can be estimated by measuring pressure drops inside the channels (p_{low} and p_{high}) and the flow rate of each feed. By subtracting the relevant pumping losses (divided by cell-pair area) to $P_{d,corr}$ yields the corrected net power density ($P_{d,net,corr}$). Full details are reported in the Supplementary Information section.

2.3.1 Tests with artificial solutions

Artificial solutions were employed to characterize the RED unit performance with known standard NaCl solutions having similar electrical conductivity of real wastewaters. First, a sensitivity analysis was performed by varying the NaCl concentration of the low salinity solution (from 0.002 M to 0.020 M) while keeping the high salinity solution concentration fixed (0.500 M). Moreover, fluid velocity of the high salinity feed was varied in order to select the most suitable fluid velocity to operate the RED unit.

2.3.2 Long-run tests

Five independent long-runs were performed by combining real wastewaters and artificial NaCl solutions as simulated wastewaters. The details of the feed solutions used in each long-run are summarized in Table 1.

The long-runs were performed as follow: each day new samples of solutions were supplied and relevant parameters were measured. Both the electrical properties of the RED unit and the feed solutions properties were monitored. In particular, as concern the latter, the electrical conductivity for the inlet and outlet samples, pressure drops, flow rates, temperature and, when applied, pH were measured. These measurements were performed under one-through feed mode (straight line in figure 2). Right after each daily test, a recirculating-feed mode was adopted, where the outlet meets the same reservoir of the inlet (dashed line in Figure 2). This feed strategy ensures a continued contact between the feed (wastewater) solutions and the membranes.

Fluid velocities for the low and high concentration solutions were 1.0 and 0.5 $cm.s^{-1}$, respectively, which resulted in a residence time inside the RED unit of 10 and 20 seconds. Only in Case V both feed velocities were 0.5 cm/s.

The backwashings were performed at inverted flow and increased fluid velocities (up to 10 cm/s) with distilled water, acid or alkaline solutions. Different concentrations of acid (HCl) and basis (NaOH) were used. Higher concentrations are expected to provide a more pronounced anti-fouling effect, but caution must be taken to avoid membrane damage. Alkaline backwashings were the ones mainly used, while the acid ones were sometimes adopted to dissolve (or to hinder) any eventual hydroxide precipitate (e.g. $Mg(OH)_2$). More details of the backwashings procedures are presented individually in the section corresponding to each long-run.

Long-run IV was carried out by imposing short and periodic inversion of current direction leading the system to shift from RED to Electrodialysis (ED) operation. These ED pulses were automated by using a suitable electrical circuit and programed with the LabVIEW interface of the National Instruments software. In particular, the ED pulses were applied for 20 seconds every 2,000 seconds. Further details are reported in the relevant section 4.1.

Note that long-run V was carried out with a fish wastewater with an increased concentration, because of a variation in the outlet stream provided by the AGS pilot plant.

Table 1: Summary of the long-runs performed in this study.

Long-run	High concentration feed	Low concentration feed	Duration
Case I	Fish wastewater (Λ=47.0 mS/cm)*	Artificial NaCl (0.004 M)	16 days
Case II	Artificial NaCl (0.500 M)	Reclaimed water (Λ=0.6-1.2 mS/cm)**	15 days
Case III	Fish wastewater (Λ=47.0 mS/cm)	Reclaimed water (Λ=0.6-1.2 mS/cm)	10 days
Case IV	Fish wastewater (Λ=47.0 mS/cm)	Reclaimed water (Λ=1.2 mS/cm)	11 days
Case V	Fish wastewater (Λ=85.7 mS/cm)***	Reclaimed water (Λ=1.2-1.8 mS/cm)****	29 days

* Roughly corresponding to 0.5 M NaCl solution.
** Roughly corresponding to 0.004 – 0.010 M NaCl solutions.
*** Roughly corresponding to 1.0 M NaCl solution.
**** Roughly corresponding to 0.010 – 0.016 M NaCl solution.

3. RESULTS AND DISCUSSION

Results are presented as follow: first, the analysis of the RED unit performance with artificial solutions is presented (section 3.1). In the following sections, results of each long-run are independently discussed. Long-runs I, II and III are devoted to the characterization of the RED unit fed by a combination of real wastewaters and artificial solutions (sections 3.2 to 3.4). In section 4 possible improvements for the process performance are tested: (i) the application of periodic ElectroDialysis pulses (long-run IV, section 4.1) and (ii) slight changes respect to the previous long-runs, i.e. mild acidification of the reclaimed water feed and decrease of v_{low} (long-run V, section 4.2).

3.1 RED unit performance with artificial solutions

The artificial NaCl solutions were used to simulate the operation with wastewaters by matching the electrical conductivity of the real solutions, i.e. NaCl 0.500 M for the fish wastewater with a conductivity of 47.0 mS/cm, and NaCl 0.004 – 0.016 M for the reclaimed water with a conductivity of 0.6 – 1.8 mS/cm. Clearly, since samples of the real wastewaters are withdrawn by the treatment processes day by day, some variations in their salinity are quite common. In particular, evaluating the effect of these variations in the overall performance of the RED system can be of paramount importance. As a matter of fact, the RED system is highly sensitive to changes in the concentration of low salinity solutions, especially when these are very low (Bevacqua et al., 2016; Galama et al.,

2014). In this sense, two parameters can be identified as the main contributing factors affecting power output when using very low concentrations: OCV and R_{low}.

The effect of lowering the diluted feed concentration C_{low} is positive on *OCV* since the potential difference given by the Nernst equation increases, but is negative on R_{low} since the solution becomes less conductive. The opposite happens when C_{low} slightly increases: a negative effect on *OCV* and a positive effect on R_{low} for the same reasons just discussed. Thus, an interplay between these two parameters does exist.

An easy way to quantitatively describe the effect of this interplay on power output is to change C_{low} over a concentration range of interest while keeping constant other experimental parameters. The range of C_{low} investigated in the present work was based on the electrical conductivity of reclaimed water samples, and consisted in NaCl solutions of 0.002 – 0.020 M, where the variations on power output can be reasonably considered as dependent on changes in R_{low} and *OCV* only. This means that small variations in IEM resistance and their effect are neglected (Galama et al., 2014). Relevant results are shown in Figure 5A: the curve has a peak obtained with a low salinity concentration of 0.012 M. By moving to the left of this maximum through the curve, R_{low} effect becomes more important than *OCV* and power density decreases because of a lower electrical conductivity in spite of a greater *OCV*. On the other side, by moving to the right of this maximum through the curve, the decrease in *OCV* is prominent compared to R_{low} contribution, and the resulting decrease in power density is due to a lower *OCV* rather than a limitation of the conductivity in the low channel.

Feed velocity is another parameter that influences power output. The use of high fluid velocity leads to high pumping losses, which affects the net power density. On the other hand, when using high feed velocity, a reduction of the non-ohmic electrical resistance results in higher power output.

The non-ohmic electrical resistance has two basic contributions: (i) concentration polarization due to the development of the Double Boundary Layer (DBL) and (ii) streamwise concentration due to the change in the salinity gradient along the fluid direction (Gurreri et al., 2014; Pawlowski et al., 2014b). Concentration polarization may significantly affect power output since the development of the DBL generates a decrease (increase) of ion concentration in the membrane/solution interface of the high (low) channel sides. Polarization effect is known to be more prominent in the dilute channel where the salinity of the feed is low, thus causing a significant reduction of the effective *OCV* (Gurreri et al., 2014).

Typical values for the feed velocity found in literature are 1 cm/s for both solutions (Pawlowski et al., 2014a; Tedesco et al., 2017), which ensures a reduction of polarization effects without producing significant power losses due to pumping the feed solutions. However, pumping losses can be particularly critical when wastewaters are used. In this regard, it was decided to test

the RED unit with v_{high}=0.5 cm/s in order to guarantee lower pumping losses and because the real concentrated wastewater was available in less amount, since the AGS-SBALR treatment is a batch process.

The analysis of the effect of feed velocity was performed with artificial NaCl solutions by setting v_{low} to 1.0 cm/s, and testing two different feed velocities for the high salinity solution (v_{high}), namely 1.0 and 0.5 cm/s. Relevant power density curves are reported in Figure 5B. As expected on the basis of non-ohmic resistance effects, the gross power density decreases when decreasing v_{high}. When considering pumping losses due to pressure drops, a rough estimation of the extent of power loss can be done by comparing the peaks of gross and net power density curves for each case: this gives a reduction of the gross power density of 6% and 4% for v_{high} 1.0 and 0.5 cm/s, respectively. This small difference is due to the fact that the RED unit is fed by artificial solutions, while larger differences are expected for the case of the wastewaters.

For this reasons, we decided to lower v_{high} to 0.5 cm/s, to further reduce power losses due to pumping, and keep v_{low} = 1.0 cm/s. The use of low feed velocities has the additional advantage of a better energy efficiency, since a major conversion of the potentially available salinity gradient into extracted power is achieved, and also results in further dilute a high salinity waste solution, which can help reducing environmental impact when discard.

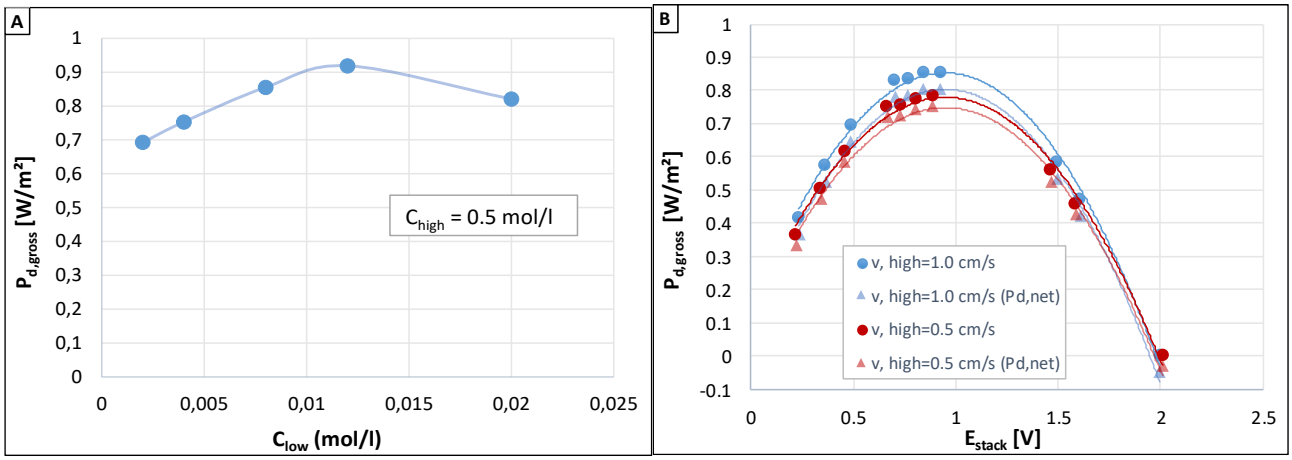

Figure 5. (**A**) Effect of the concentration of low salinity solution on power density, using a fixed value C_{high} = 0.500 mol/l and feed velocities of v_{high} = 0.5 cm/s, v_{low} =1.0 cm/s, lines connecting the points are added to guide the eye. (**B**) Power curves as a function of v_{high} at fixed v_{low} = 1.0 cm/s and C_{high} = 0.500 mol/l, C_{low} = 0.004 mol/l. Pressure drops were 0.01 bar (v_{high} = 1.0 cm/s) and 0.007 bar (v_{high} = 0.5 cm/s).

3.2 Long-run I: Real fish wastewater / artificial low salinity solution (NaCl 0.004 M)

The first long-run combined real fish wastewater, as the high salinity solution, with artificial low salinity solution at concentration 0.004 M NaCl (based on the conductivity of the first samples collected of reclaimed water). Figure 6 shows the time evolution of key parameters measured during the sixteen days of duration of the long-run. Plots are organized as follow: Figure 6A shows the time evolution of stack resistance together with pressure drops, Figure 6B depicts gross and

corrected net power density over time, and Figure 6C shows the OCV_{exp} and the apparent permselectivity, α_{app}.

As it can be seen, the trend of the net power density follows a positive, yet decreasing response during the first week of measurements, and a negative value starting on the 8th day due to the development of fouling. Basically, the progressive increment of pressure drops and of stack resistance (Figure 6A) turned the balance between power produced and power required for pumping the solutions (Figure 6B). Thus, when the net power output was found to be negative, a series of cleaning procedures were tested in order to reverse fouling.

Note that inside the high channel the increment in pressure drops is more evident since it is fed by wastewater. The low channel also experiences an increment in pressure drops, due to the progressive increase in the adjacent (high salinity) compartments, and it is noticeable given the higher fluid velocity of the low channel (1.0 cm/s in the low vs. 0.5 cm/s in the high). The increase in p_{low} was not expected since pure NaCl solution was used as feed. Comparison of both trends (p_{low} and p_{high}, Figure 6A) indicates that this increase was somehow produced after pressure drops in the high channel increased, probably due to membrane deformation or due to some additional concentrated pressure losses (caused by pressure increase in the high channel).

First, fouling has an effect on pressure drops, and second on stack resistance, as it can be seen in Figure 6A. Pressure drops start to increase early in the long-run, particularly starting on the 5th day (probably sooner, during the weekend) while stack resistance is somehow constant until the 8th day, where a marked increase is observed. The early detection of increase in one of them (pressure drops) and the delay in the other (R_{stack}) distinguishes between two stages of the fouling process. In the first stage, the presence of sub-micro particulate in the feed wastewater (<5 μm) leads to partial obstruction of woven spacers and thus increasing pressure drops. Parallel to the obstruction of spacers, sub-micro and (macro) molecular-size pollutants start to adsorb on the surfaces and/or to permeate inside the membranes. At the beginning, the effect of adsorbed pollutants on the overall performance is negligible, until the progressive accumulation leads to an increase in R_{stack}. The presence of a significant amount of pollutant, either deposited over the membranes surfaces and/or blocked inside the membranes, interferes with ion transport, thus leading the electrical resistance to increase.

3.2.1 Cleaning effects and fouling identification

Given the composition of the fish wastewater, it was expected that fouling, if produced, would be mainly of organic or biologic nature based on COD and BOD indexes of the fish wastewater feed (Figure 3). Previous works found clay deposits in the feed spacers and organic fouling when using river water as feed in Reverse ElectroDialysis, which caused an increase in pressure drops

(Pawlowski et al., 2016; David A. Vermaas et al., 2014a; Vermaas et al., 2013). Kingsbury et.al. remarked the role of organic fouling in RED when using real waters and wastewaters (Kingsbury et al., 2017); in addition, biofouling due to the adsorption of bacteria on ion exchange membranes can occur in RED (Vaselbehagh et al., 2017).

The adsorption and transport of organic species in IEMs depends more on its charge and size, and its hydrophobic and aromatic features, rather than on its concentration, a behaviour that is reported for ED (Lee et al., 2003; Vanoppen et al., 2015) and RED experiments (Kingsbury et al., 2017). As remarked in these works, organic fouling is produced preferentially in the dilute side and affects particularly AEMs. In the diluted channel, the osmotic flux, the concentration profile and the larger double boundary layer thickness may be responsible in concentrating organic matter at the membrane interface and thus promoting its adsorption. Furthermore, the intensity of the current density seems to be irrelevant in this process: the transport of organic molecules is mainly diffusion-driven, and is disadvantaged by the increase in salinity and the magnitude of the current density (Vanoppen et al., 2015). Seemingly, the current density in RED conditions (slightly) disfavours bacteria adsorption on AEMs (Vaselbehagh et al., 2017).

The aspect of the membranes after the long-run (Figure 6D) show that AEMs were brown dyed, while no perceptible changes was observed in CEMs, a result consistent with the preferential bio- and organic fouling on AEMs found in literature (Lee et al., 2009; Vaselbehagh et al., 2017). Indeed, it is strongly suspected that both types of fouling were produced in this case: the AEMs appearance after the long-run and the effectivity of the alkaline backwashing suggests the presence of organic fouling, while the increase of stack resistance during the second weekend, after the neutral backwashing, can only be explained by the presence of biofouling, as it will be explained in the following.

The first backwashing was with distilled water (neutral backwashing in Figure 6A), with the intention of physically remove foulants by increasing fluid velocity. The procedure consisted in the application of higher feed velocities for short times (ca. 5 minutes) and afterwards measuring the pressure drops at normal feed velocity. This procedure was repeated by applying further short steps of backwashings with progressively higher feed velocities (up to 3.o cm/s) until the measured pressure drops were the closest they could be to their initial values.

Since the values of pressure drops were still high after the neutral backwash, the long-run was partially stopped and the RED unit was kept with artificial NaCl solution during the weekend. After the weekend, distilled water was flushed at normal fluid velocities. Surprisingly, pressure drops in the high channel were even higher than before the neutral backwashing. This clearly indicates that the source of this new increment in p_{high} was produced inside the RED unit during the weekend and not from an external feed source, thus suggesting the presence of bacteria on the membranes

surfaces that growth during the weekend. This fact is also supported by the invariance of p_{low} during the weekend.

Bacteria growth was possible even if the fish wastewater was acidified before feeding the RED unit because the artificial NaCl low salinity feed is neutral. As protons easily permeate IEMs, the pH of the fish wastewater rapidly raises above 6.0 and remains like this under recirculating feed mode, which allows bacteria to develop more easily. When the RED unit was left in a bath of salty solution during the weekend, remaining clusters of strongly adsorbed bacteria could grow freely.

At this point and after the neutral backwashing, chemical backwashings were performed. First, an HCl solution of pH=4.0 was tested, which was effective in lowering p_{high} but not p_{low}. Since pressure drops after the acid cleaning were similar to those obtained after the neutral backwashing, an alkaline backwashing with a NaOH solution of pH=9.0 was implemented, which succeeded in lowering p_{low} while a further decrease in p_{high} was observed, corresponding with the preferential fouling in AEMs.

Besides a decrease in pressure drops, the sudden effect of chemical backwashings seemed to be an increase in the stack resistance (11^{th} day in Figure 6A). This is not clear since no measurements could be performed just before the chemical backwashings due to the high pressure drops, and it is very possible that the electrical resistance right before the backwashings was indeed higher. With respect to this, an increase in the electrical resistance of IEMs after chemical cleaning was found by Pawlowski et al. (Pawlowski et al., 2016). In their work, the RED unit was unmounted after a long duration experiment and the membranes were washed with concentrated chemical reagents. They attributed this increase to the degradation of charged sites and polymeric chains scission (Garcia-Vasquez et al., 2016) of the heterogeneous IEMs they used. In comparison, in this work the chemical backwashing was applied *in situ* and the membranes were dense polymeric homogeneous IEMs. It is unlikely that the acid and base solutions could severely damage the membranes since the concentration of H^+ and OH^- was very low, within the range suggested by the manufacturer, and the time of exposure was limited. Most probably, the high value of R_{stack} would be representative of the fouling conditions of the RED unit moments before performing the backwashing. This is confirmed by preliminary tests performed in a RED unit assembled with a clean set of membranes and fed with artificial solutions only, where no changes of R_{stack} before and after the chemical backwashing, were observed.

The day after the backwashing (12^{th} day), R_{stack} was restored to its initial value, a result that suggests that no significant membrane deterioration took place. The fact that the OCV and perm-selectivity remain constant throughout the long-run (Figure 6C) also supports this idea. The effect of the chemical backwashings did not last for long since both pressure drops and R_{stack} increased again, this time much faster than the first week. It is suspected that bio- and organic fouling was

very advanced at this point, and that strongly attached remaining foulants that were not able to be removed caused the faster detriment. The presence of foulants after the cleaning procedures is clear, and explains the faster increase of the electrical resistance observed in the following days. The brownish aspect of AEMs after the long-run, Figure 6D, also indicates the presence of remaining foulants and suggests that fouling is at some extent irreversible, although no additional cleaning cycles were tried, that could further remove foulants. It is not possible to state which kind of fouling, biologic or organic or both, is the responsible for the process irreversibility, but it is suspected that organic molecules blocked inside the membranes and/or strongly adsorbed at the membrane surfaces, were responsible for the irreversible fouling. In this sense, an earlier and more frequent application of alkaline backwashings should be a good strategy for prevention of fouling phenomena produced by the fish wastewater.

3.2.2 RED unit performance and power output

One of the main advantages of using wastewaters as feed solutions for power generation is their otherwise null value. In particular, high salinity wastes represent an actual environmental challenge, which makes RED an appealing technology that could handle two major issues: valorisation of waste by direct clean-energy production, and reduction of environmental impact by diluting this kind of wastewaters.

In order to make this process feasible, two main aspects should be addressed. First, the durability of the RED unit(s) should be consistent with the installation costs and the power produced for the time that is operated, meaning that the power produced should be high enough and, most importantly, able to endure long enough in order to justify the initial investment. Second, the balance between power consumed and power generated must be positive. A versatile RED installation that alternates between diverse kinds of feeds, either of artificial, natural or waste origin, may be a way to help this assessment, with a strong dependence on system maintenance over time.

The first aspect concerning power produced is illustrated in the trend of gross power density, represented by blue marks in Figure 6B. As briefly mentioned early, the trend follows a steady response during the first eight days of experiment, after which accumulation of pollutants and development of fouling decreased the performance.

The first values of $P_{d,gross}$ are comparable to those obtained with artificial river and seawater (Veerman et al., 2009), which have similar levels of salinity as the feeds used in this work, and are consistent with the common values reported in literature with artificial solutions (Hong et al., 2015). A maximum power density of 0.87 W/m^2 was obtained in the sixth day. The lowest values were 0.57 and 0.61 W/m^2, corresponding to the twelfth and sixteenth days of the long-run, respectively, when the stack resistance was the highest. This indicates that the main detriment of fouling on

power output, besides pumping losses, is the increase of the electrical resistance. Indeed, chemical cleaning helped in restore initial power output up to 0.81 W/m^2 reported the day after the backwashings (due to a decrease in stack resistance) but R_{stack} increased rapidly in the following days because of remaining foulants, and gross power density decreased again.

A more realistic analysis for possible future scale-up of a RED unit requires the subtraction of the blank resistance (which in this long-run represented more than 30% of R_{stack}) and the evaluation of pumping losses. Resulting $P_{d,corr,net}$ values are reported as red triangles in Figure 6B.

The first values of $P_{d,corr,net}$ were around 1.50 W/m^2 which are consistent with the values obtained with pure artificial NaCl solutions (Figure S2B in Supplementary Information section). In the following days, a progressive decrease was observed mainly due to pumping losses, which started early in the long-run in correspondence with the trend in pressure drops. Chemical cleaning helped in decrease pressure drops, and a reasonable positive value was obtained in the 13th day. This condition did not last long, and $P_{d,corr,net}$ decreased again, more rapidly to negative values mainly due to the increment of pressure drops.

The overall RED performance and the effect of fouling can be observed in the results of spot tests carried out with artificial NaCl solutions that were taken on the first, eighth and sixteenth days (green spots in Figure 6). Absolute values of R_{stack} of the spot tests were 10.7, 12.9 and 13.1 **Ω** respectively (Figure 6A) indicating an increase in electrical resistance due to fouling, which affected gross power density (0.78, 0.73 and 0.72 W/m^2, Figure 6B). Electrochemical properties of ion exchange membranes were not severely affected by fouling as suggested by the invariance of *OCV*: 2.01, 2.00 and 2.02 V and a nearly constant value of the estimated permselectivity, α_{app}: 0.90, 0.87 and 0.88 (Figure 6C). Last, no changes in the inlet and outlet temperature were observed in the duration of the long-run as expected.

3.3 Long-run II: Artificial high salinity solution (NaCl 0.5 M) / real reclaimed water

The second long-run combined treated civil wastewater (usually known as reclaimed water), as the low salinity solution, with an artificial high salinity solution of NaCl 0.5 M. Procedures for this long-run were the same as before and the results were similar to the previous case. As expected, the electrical resistance throughout the long-run was lower, allegedly due to the slightly higher electrical conductivity of the reclaimed water feed, while pressure drops increased at nearly the same rate (Figure 7A).

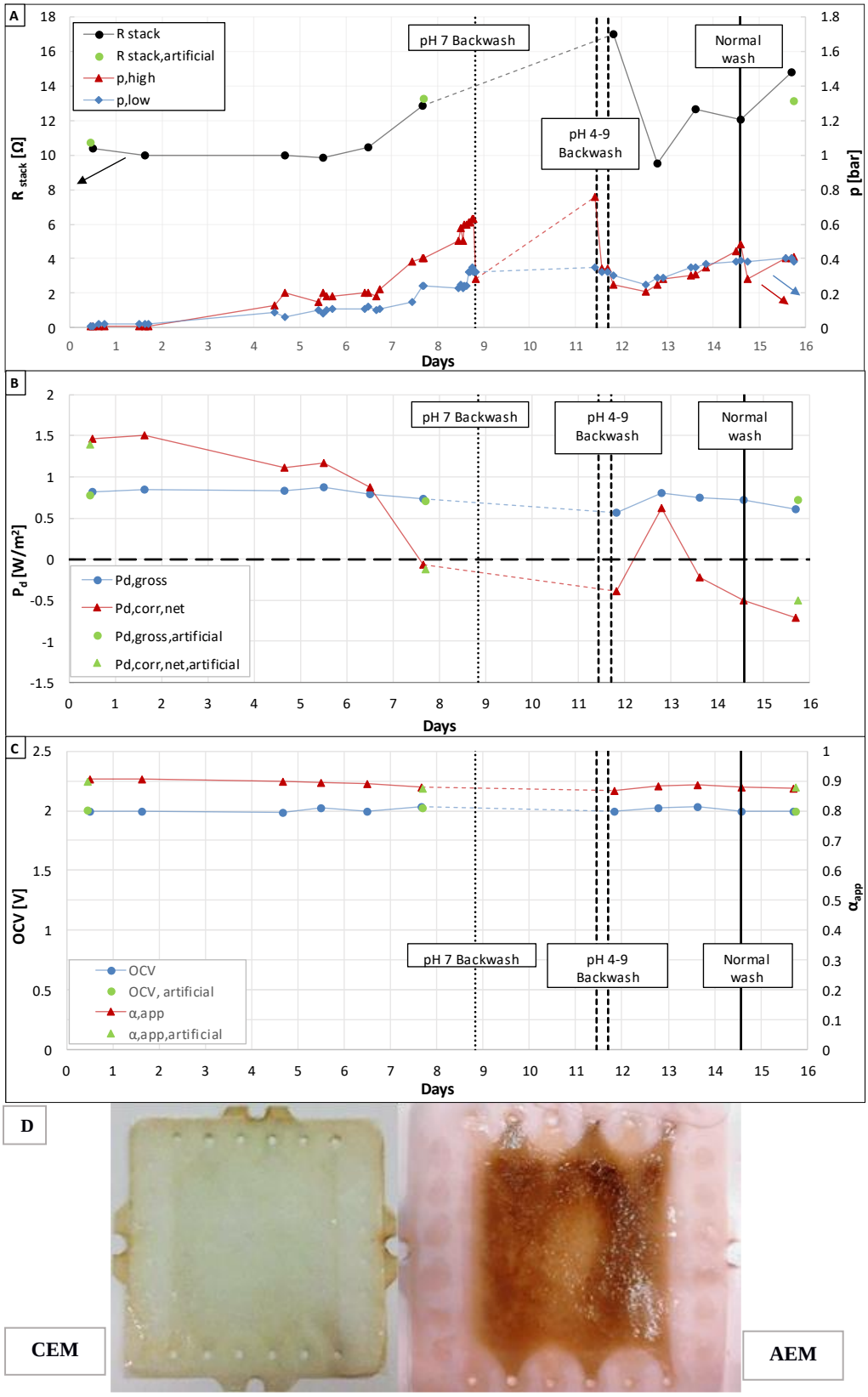

Figure 6. Time evolution of selected parameters for long-run I showing: (**A**) Pressure drops for the high and low compartments and R_{stack}; (**B**) Maximum gross and corrected net power density; (**C**) Open circuit voltage and apparent perm-selectivity; and (**D**) Pictures of ion exchanges membranes after the long-run. Spot test with artificial solutions are shown in green (●); back washings are indicated with vertical lines.

In particular, small variations were found in the electrical conductivity values of the reclaimed water samples that were periodically collected. As previously discussed, these small variations have a strong influence in the RED unit since the low salinity conductivity is a dominant component of the total electrical resistance (section 3.1). Thus, in order to clarify the analysis, electrical conductivity values of the reclaimed water sample that were used in each day are reported in the graphs of Figure 7.

The increase in pressure drops and later on stack resistance, produced as a consequence of membrane fouling, progressively decreased the net power output, giving the first negative value on the eighth day. However, the negative effect of fouling due to the reclaimed water was softer in comparison with the fish wastewater, since no acid or base was needed to clean the RED unit, and a better net power density was maintained until the end of the long-run (Figure 7B). No severe detriment of the ion-exchange capabilities of membranes was observed after the long-run as suggested by the invariance of the permselectivity (Figure 7C). Fouling was mainly of organic nature and affected exclusively AEMs, while no perceptible changes where observed in CEMs (Figure 7D).

3.3.1 Cleaning effects and fouling identification

The raw civil wastewater was treated in a MBR system before using as feed, and the result is a low turbidity feed with low content of organic load. Particulate of size larger than 0.04 μm is rejected by the ultrafiltration module of the MBR (Cosenza et al., 2013; Hirani et al., 2013) and thus no further filtration steps were applied. Therefore, potential foulants were small organic (macro) molecules, inorganic forms of phosphorus and nitrogen, inorganic cations that could precipitate and produce scaling, and biofouling by algae growth.

The risk of biofouling due to algae growth was avoided by covering tanks, pipes and the RED unit from light exposure. This was successful for the two weeks of operation since no traces of algae were found in the feed spacers and no sign of biofilm was found over the membrane surfaces after the long-run. However, algae proliferation did occur much later. The membranes that were used in this long-run were carefully and thoroughly washed with distilled water and kept in sealed tappers, AEMs and CEMs separately. After six months it was visually evident the presence of algae only in the tapper containing AEMs. In order to grow, algae need phosphates and nitrates, which in consequence were present in the membranes surfaces and/or inside them. This suggests that, although no chemical cleaning was performed during the two weeks, it could be positive to apply chemical backwashing from time to time in longer operations.

On the other side, inorganic scaling by multivalent cations was not observed, either directly or

indirectly, although more detailed analysis should be performed to confirm its inexistence. In ion-exchange membrane processes, precipitation of hydroxides preferentially in CEMs is possible in alkaline environments or in the presence of carbonates, in particular when water splitting takes place or in applications such as the alkaline fuel cells (Mikhaylin and Bazinet, 2016), but since the pH of the feeds was always neutral, this hardly occurred. For this reason, it is believed that, if occurred, scaling was irrelevant.

As mentioned before, concentration of organic molecules is favoured in the low salinity channel due to DBL effects and due to the osmotic flux, which promote their adsorption (Kingsbury et al., 2017; Lee et al., 2009). It is also possible that organic molecules present in the diluted side may be able to be transported to the concentrated side, i.e. against the salinity gradient direction, since the transport of organic molecules is mainly diffusion driven and where a fraction of the adsorbed and transported molecules may remain stuck in the membrane (Kingsbury et al., 2017; Vanoppen et al., 2015). Indeed, visual inspection of the membranes after the long-run showed a dark brownish dyeing of AEMs with very similar appearance of that found by Pawlowski et al. (Pawlowski et al., 2016) (Figure 7D), where organic fouling was determined in AEMs, presumably due to humic compounds present in the river water. These results clearly indicate the presence of negatively charged species that attach to AEMs.

The effect of organic fouling was an increase in pressure drops, and later an increase in stack resistance, the same result as in the previous case. Pressure drops started to increase very early in the low channel, where the real wastewater was fed, followed by a progressive increment in the next days (Figure 7A). The increase in p_{low} led to an increase in p_{high}, which at the end of the first week was even higher than p_{low}. Similar to the results of the first long-run, the increase in pressure drops of the concentrated channel is somehow linked to the p_{low} increase: when examining the trends of pressure drops right after the backwashing (days 11^{th}-13^{th}), p_{high} shows a steady response and only increases the day after an increase in p_{low} is produced.

Eventually, fouling affected also the electrical resistance of the RED unit. A direct comparison of R_{stack} values cannot be done without accounting for the electrical conductivity of the reclaimed water sample that was used in a particular measurement. With this consideration, the increase in R_{stack} can be observed in the seventh and eighth day, where the electrical conductivity of reclaimed water was the same and a clear increase of electrical resistance was produced.

On day 11^{th} a neutral backwashing was performed with a slightly different procedure than in the long-run I. It consisted in back-feeding the RED unit with distilled water, by applying higher fluid velocities that were progressively increased (every 30 seconds) up to 3 cm/s, and then lowering it to normal fluid velocity. This procedure was repeated five times, after which a significant decrease in pressure drops was observed. Besides physically remove foulants, the high

flow rate may carry air bubbles that could help in removing organic matter from the membranes, an anti-fouling strategy that was proof to be effective in RED (Vermaas, et al., 2014a). The neutral backwashing achieved an instantaneous decrease in pressure drops and a decrease in R_{stack} observed the next day.

After the backwashing, p_{low} showed a value of 0.18 bar that increased again up to the end of the long-run, while p_{high} showed a value of 0.10 bar that was maintained stable for three days, after which it increased again as a consequence of p_{low} increment. Furthermore, R_{stack} was fully recovered to its initial value, suggesting that in this case fouling was at some level reversible: the spot tests with artificial solutions that were performed during the long-run illustrate the invariance of R_{stack}, where the same value was obtained in the first and last spot tests, and a higher value was obtained in the eighth day when fouling was the highest.

3.3.2 RED unit performance and power output

In general terms, the system performance was better than the long-run with fish wastewater due to the softer effect of fouling in this case. Overall, the RED unit was able to produce a constant gross power density during the two weeks of experiment, with the exception of the decrease when membrane fouling was the highest.

The highest gross power density produced with reclaimed water was 0.79 W/m^2 obtained in the twelfth day (Figure 7B), while all other values were similar and consistent with those obtained with artificial solutions reported in literature (Hong et al., 2015). When membrane fouling evolved and produced an increase in R_{stack}, power was clearly affected, but this was able to be reversed with the neutral backwashing. Conversely, pressure drops were the most detrimental factors of power output, as indicated by the $P_{d,corr,net}$ trend. A negative balance between power produced and power consumed was obtained in the eighth day, in correspondence with the maximum of pressure drops. The neutral backwashing significantly decreased pressure drops, turned this balance, and positive values of $P_{d,corr,net}$ were obtained in the following days, practically up to the end of the long-run.

The values of *OCV* (Figure 7C) were consistent with the expected values: when the electrical conductivity was higher, the *OCV* was slightly lower, and vice versa. A clear decrease of *OCV* was observed when membrane fouling was the highest, probably due to the presence of adsorbed molecules at the interface. However, since after the neutral backwashing the *OCV* was restored to its initial value, it is clear that the backwashing was able to remove some of the loose-bonded, superficial foulants. Moreover, and regardless of the low salinity feed used (reclaimed water or NaCl solution), the apparent permselectivity was invariant during the long-run, with estimated values of 0.88-0.91. These values of α_{app} were also consistent with those obtained in the first long-run, as expected given the same kind of membranes that were used.

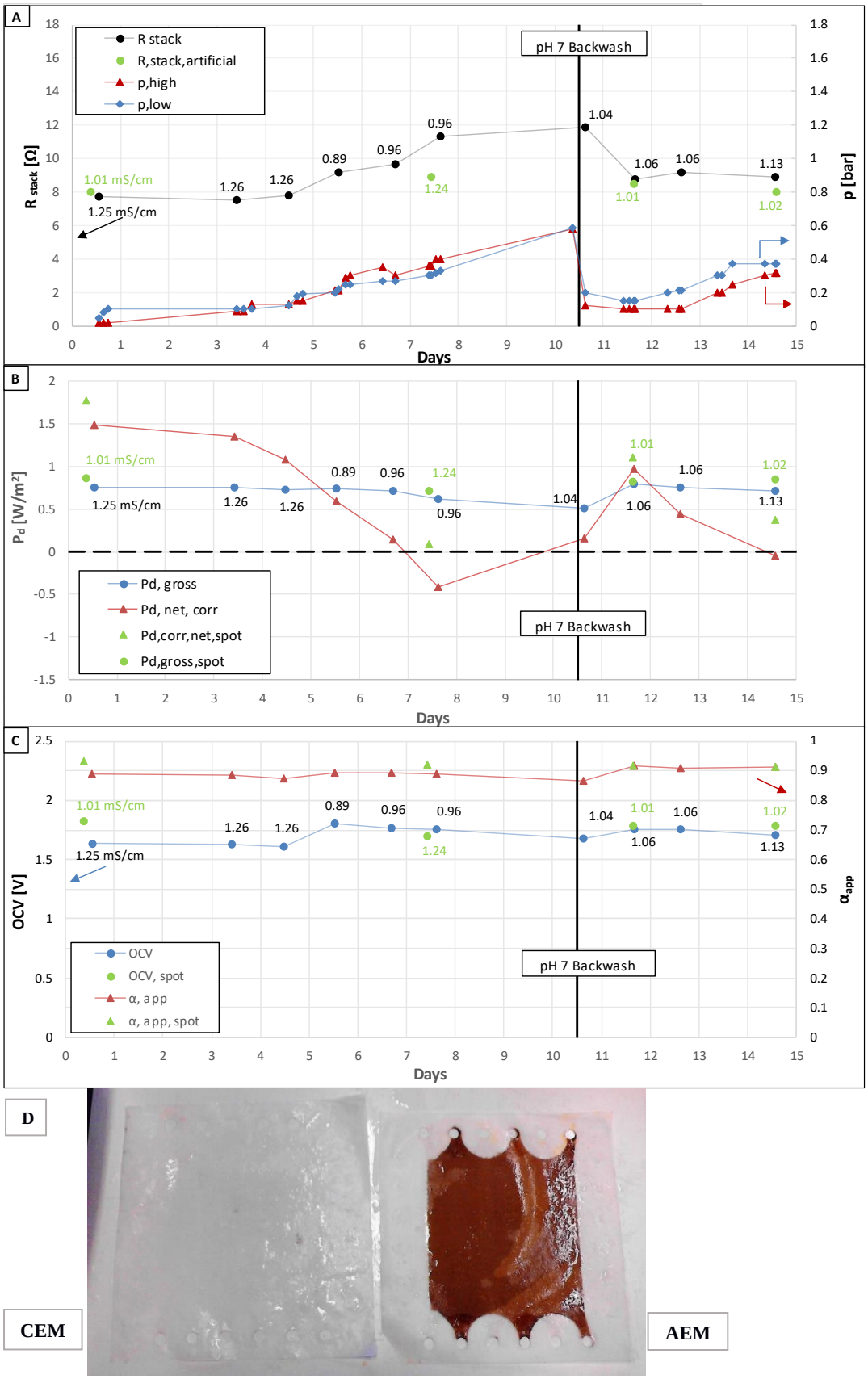

Figure 7. Time evolution of selected parameters for long-run II, showing: (**A**) Pressure drops for the high and low compartments and R_{stack}; (**B**) Maximum gross and corrected net power density; (**C**) Open circuit voltage and apparent perm-selectivity; and (**D**) Picture of IEMs after the long-run. Tests with artificial solutions are shown in green (●); neutral back washing is indicated with a vertical line. Conductivity values (mS/cm) of inlet reclaimed water samples are reported as labels.

3.4 Long-run III: Real fish wastewater (high) / real reclaimed water (low)

This case combined both wastewaters as feed solutions, the results of time-evolution of selected parameters is presented in Figure 8. The general trend shows a faster detriment due to membrane fouling caused by the composition of both wastes. Stack resistance was higher in comparison with the previous long-runs, and hence the gross power density obtained throughout the long-run was lower. The *OCV* and the apparent permselectivity were affected by membrane fouling, a result that was not observed in the previous long-runs.

Cleaning procedures consisted in two alkaline backwashings, based on the organic fouling observed in the previous long-runs and the preferential fouling in AEMs. The backwashing was effective in partially recover system performance, as observed in the recovery of power density and also of the *OCV* after the second cleaning, although the general features of the RED unit decreased with respect to its initial response.

The long-run was stopped some days before than planned given the advanced state of fouling. The main type of fouling was presumed to be organic and affected exclusively AEMs, as suggested by the appearance of the membranes after the long-run and based on the results of the previous cases. No signs of biofouling were detected as it was observed in the first long-run, very likely due to the early application of the chemical cleaning, which could have acted as prevention of bacteria growth. Similar as in the previous long-runs, the effect of fouling was an increase in pressure drops and very early (4^{th} day) in the stack resistance (Figure 8A). The increase in pressure drops was slightly higher in the low channel, which is consistent with the higher fluid velocity of the reclaimed water. Given that pressure drops and R_{stack} rapidly increased, and that P_d and *OCV* decreased from their initial values, an alkaline backwashing with a NaOH solution (pH 9) was performed on day 5^{th}, before the weekend. Backwashing procedures were the same as for the long-run II. The cleaning was able to decrease pressure drops and thus allowed us to continue feeding the RED unit during the weekend, but no changes in R_{stack} were observed right after the first backwashing. During the weekend, p_{low} continued to increase while p_{high} remained constant, a result consistent with the concentration and accumulation of organic matter near the surface of AEMs in the diluted side. Based on the still high values of pressure drops, a second alkaline backwashing with a more concentrated NaOH solution (pH 11) was performed. A further and more effective decrease of pressure drops was achieved, but no immediate changes on R_{stack} were observed. Instead, the electrical resistance decreased on day 10^{th}, i.e. 48 hours after the chemical cleaning.

3.4.1 RED unit performance and power output

The average power density generated by the RED unit was lower than the previous long-runs, Figure 8B. A maximum $P_{d,gross}$ of 0.66 W/m^2 was obtained in the second day, after which it further

decreased due to membrane fouling. Values of the corrected net power density, with a maximum of 0.77 W/m^2 obtained in the first day, were lower in this case since the electrical resistance was high, and thus R_{blank} had less weight in the correction of $P_{d,gross}$. The alkaline backwashings were successful in keeping low levels of pressure drops, reversing $P_{d,corr,net}$ and achieving a positive balance of generated/consumed power by the end of the long-run.

The lower performance of the RED unit was related to the organic fouling produced on both sides of AEMs and the higher values of R_{stack}. In the long-run I, the low electrical conductivity of the diluted feed produced relatively high values of electrical resistance, but this was compensated by a higher *OCV*. In the long-run II the electrical conductivity of the reclaimed water was slightly higher and hence the average values of R_{stack} were smaller, in spite of a lower *OCV*. Overall, the effect of one parameter was compensated by the other, thus producing similar power output in both previous cases. In this third long-run, the electrical conductivity of reclaimed water samples was similar to those of the second long-run: indeed, the firsts values of *OCV* of this case match with those of the second long-run (Figure 8C), but R_{stack} was higher this time, and this was the reason for a lower power density.

The comparison of the RED unit features obtained with real wastewater, with those obtained in the spot tests with pure NaCl solutions, is somehow difficult given the changes in the electrical conductivity of the reclaimed water, although in general the spot tests gave better results. In this sense, a more trustable comparison can be done by comparing the power produced in this long-run with that produced in the previous long-runs, which shows an average decrease of 20% in $P_{d,gross}$. This is clearly an effect of fouling in both sides of the membranes. Also, this decrease can be related to the presence of divalent ions Ca^{2+}, Mg^{2+} and SO_4^{2-} present in both feeds, that can affect power density from 30% to 60% depending in their concentration (Avci et al., 2016; David A. Vermaas et al., 2014c), and can also increase the electrical resistance due to higher electrostatic interactions with the fixed charge groups of IEMs (Badessa and Shaposhnik, 2016, 2014). In this regard, it is not clear if the effect of multivalent ions is more pronounced if they are present in both feeds; apparently from the results of this work this effect is somehow reduced if multivalent ions are present only in one of the feed solutions.

Together, these results and those of the previous long-runs show the softer effect of using only one wastewater combined with pure NaCl solutions, and a more pronounced detriment when both wastewaters are used as feed solutions in a lab-scale RED unit.

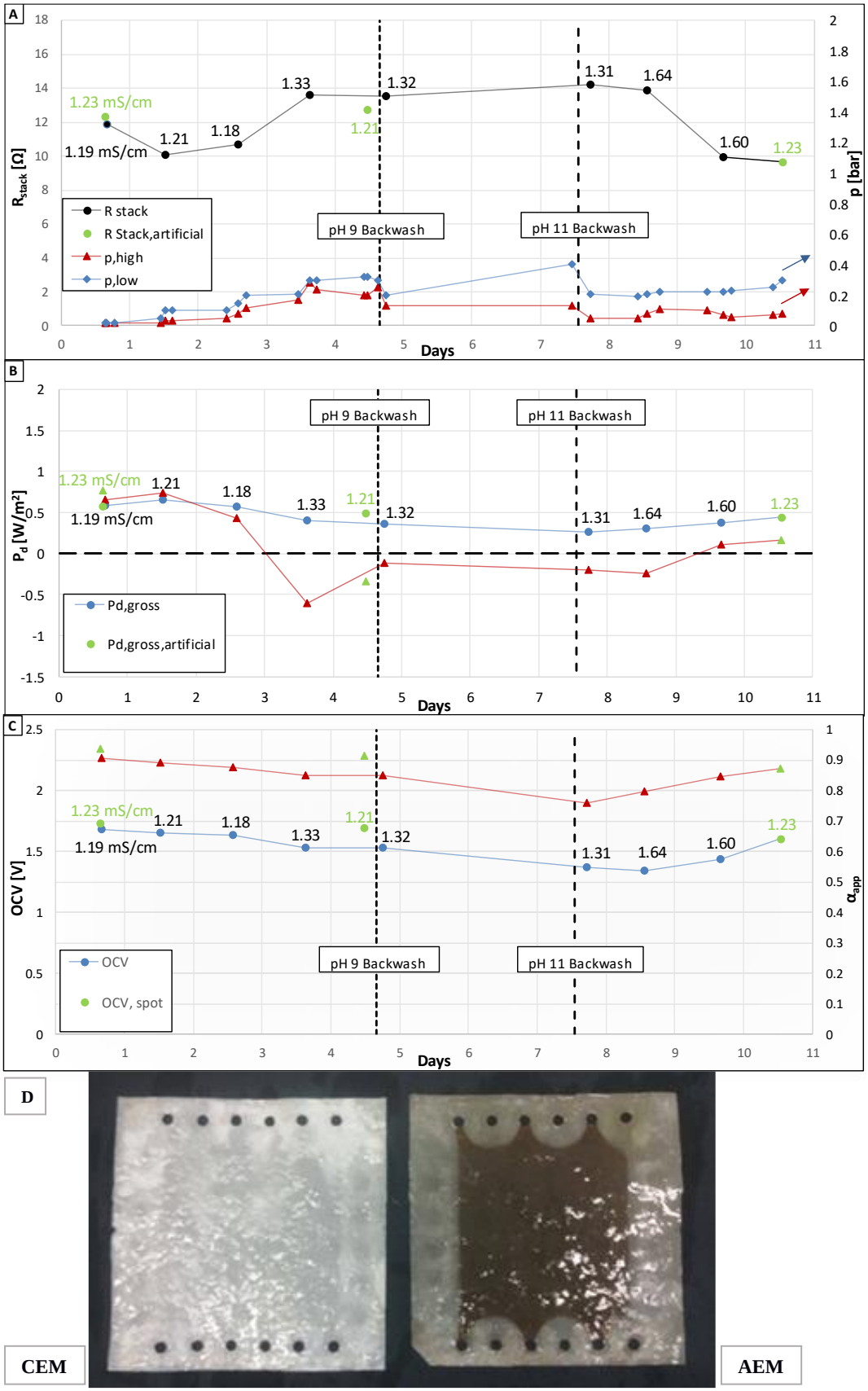

Figure 8. Time evolution of selected parameters for long-run III, showing: (**A**) Pressure drops for the high and low compartments and R_{Stack}; (**B**) Gross and corrected net power density; (**C**) Open circuit voltage and apparent perm-selectivity; and (**D**) Picture of ion exchange membranes after the long-run. Spot test with artificial solutions are shown in green (●), backwashings are indicated with vertical lines. Labels correspond to the inlet conductivity values (mS/cm) of reclaimed water samples.

4. POSSIBLE STRATEGIES TO IMPROVE SYSTEM PERFORMANCE

Two more long-runs were performed based on the results of the previous ones, both of them used real wastewaters as feeds and focused on the improvement of the process performance. In the long-run IV a periodic application of ElectroDialysis pulses was adopted in order to analyse its effect as membrane-fouling prevention strategy (section 4.1). In the long-run V some adjustments were applied in the wastewater feeds (section 4.2).

Backwashing procedure in these cases was further tuned based on the observations of the previous long-runs: it consisted in back feeding the RED unit with the cleaning agent (acid or base) at lower fluid velocity (<0.5 cm/s) with interposed stops, so to leave the cleaning agent to act for a while, and it was finished when the outlet pH was the same as the inlet. This procedure usually consumed 5 L of cleaning agent and lasted about 60 minutes. Right after the chemical cleaning, a physical back-cleaning with distilled water was applied, starting with normal fluid velocities (0.5 cm/s) and increasing it step-by-step as in the previous long-runs (i.e. up to a maximum fluid velocity of 3.0 cm/s). In addition to the backwashings, when pressure drops were found to be high during the course of the long-runs, short consecutive pulses (1-2 seconds) were also applied at the maximum flow rate allowed for the peristaltic pump (corresponding to about 10 cm/s). These flushings may prevent the passive sorption of foulants over the membranes surfaces, promote their desorption and physically unclog the feed spacers. The choice of using short consecutive pulses instead of a single longer one comes from the literature. In particular, Moreno and co-authors (Moreno et al., 2017) showed that the consecutive application of air and/or CO_2 injection in series of 3x2s were much more effective than the application of a single perturbation of 1x6s.

4.1 Long-Run IV: ElectroDialysis-Pulses

The use of reversed electrical pulses is a common anti-fouling practice in ElectroDialysis (ED) applications. By inverting the current density direction, the (charged) foulants that accumulate over the membrane surfaces can be desorbed thanks to the inverted ion flux that is produced. In ED this is usually accomplished by reverting the electrodes polarity at regular intervals (ElectroDialysis Reversal, EDR) (Katz, 1979) or by the application of Pulsed Electric Fields (PEF), in which the power supply is periodically switched off at suitable intervals (Lee et al., 2002; Lee and Moon, 2005; Ruiz et al., 2007). On the other side, in RED operation, ion transport occurs spontaneously from the high to the low salinity compartments, thus, to achieve an inversion of the ion flux it is necessary to apply an overpotential higher than the defined OCV in order to force the ions to move from the diluted to the concentrated side (i.e. corresponding to desalting operation as in classic ED). The magnitude of the overpotential has to be chosen such as not to exceed the limiting current density (i_{lim}) and avoid dramatically high electrical resistance values. Values for i_{lim} mainly depend

on the (low salinity) feed concentration, the stack geometry, the fluid velocity and on the ion exchange membranes material and features (Lee et al., 2006). In general terms, higher concentrations and faster fluid velocities exhibit higher values of limiting current density (Tanaka, 2005). According to the experimental stack (e.g. membrane and spacer features) and experimental conditions investigated (e.g. $C_{low} \approx 0.01$ M and a feed velocity $v_{low} = 1.0$ cm/s), the limiting current density value can be derived from the literature for a very similar system (Tanaka, 2005) and reasonable considered to be about 10 mA/cm^2. Therefore, pulses were conservatively performed with a potential of 3.25 V (higher than OCV=1.60 V) corresponding to a current density of 2 mA/cm^2.

When a sudden current inversion is applied, a certain response or relaxation time (τ) is required to effectively reach a net ion flux in the opposite direction. This is due to many factors such as the inertia of transported matter and the time required for the change in the concentration polarization profiles. According to Vermaas et al. (David A. Vermaas et al., 2014b), this time depends on the transport mechanism inside the channels. At low direct (i.e. ED mode) current densities ($i << i_{lim}$) electro-convection effects can be neglected (Rubinstein and Zaltzman, 2000). The woven spacers employed promote mixing by increasing the convective contribution of the overall convective-diffusive transport (Gurreri et al., 2016). As a matter of fact, at the Reynolds number investigated (about 6) resulting transport is predominantly convective, being the Sherwood number equal to about 30 (Gurreri et al., 2016). According to the empirical estimated provided by Vermaas et al. (David A. Vermaas et al., 2014b), under mainly convective transport, τ can be assumed to be proportional to the average residence time of the feed. Following these assumptions, Vermaas and co-authors (David A. Vermaas et al., 2014b) reported a response time $\tau \approx 4$s when switching from RED to ED operation for a system with a flow rate of 50 ml/min and with feeds concentrations similar to the ones used in this work. In contrast, the flow rate of the dilute solution in the present long-run was more than three times higher (160 ml/min), thus a slightly lower τ would be expected. On the other hand, (David A. Vermaas et al., 2014b) also found that the response time increases when feed channels are partially obstructed, as it happens in the present case. With these considerations, the current pulse time was set at 20 seconds (i.e., five times higher than the τ reported by Vermaas et. al.) to ensure an inverted ion flux for a reasonable time. These ED pulses were applied periodically every 2,000 seconds, such that only 1% of the time the RED unit operation was interrupted by the ED pulses.

The time evolution of the selected parameters is shown in Figure 9. Since the objective of this long-run was to evaluate the effect of the ED pulses in R_{stack}, a sufficient amount of reclaimed water coming from the MBR pilot plant was accumulated and stored to avoid changes in the electrical conductivity ($\Lambda = 1.2$ mS/cm) along the long-run, thus ensuring that eventual changes in R_{stack} are

not produced by changes in the reclaimed water salinity.

The main difference with respect to the other long-runs concerns the R_{stack} trend (Figure 9A), which was found to be somehow constant with time with a mean value of (9.4±0.5Ω). This result illustrates the effectivity of the ED pulses in preventing the progressive accumulation of pollutants over the membrane surface, thus allowing membrane fouling to be controlled. This finding is also confirmed by the practical constancy of $P_{d,gross}$ over time (mean value equal to 0.65±0.06 W/m^2, Figure 9B) and by the AEMs appearance (Figure 9D) which looked much cleaner in comparison with the previous cases. On the other hand, Figure 9A, also shows a dramatic pressure increase, especially in the concentrate channel, thus suggesting that in this case the channel clogging due to physical obstruction of feed spacers is the main detrimental factor of system performance. These clogging issues were somehow addressed by the use of the chemical backwashings which were found able to reduce the pressure in the channels, although a general increasing trend is however observable (Figure 9A). This has a direct effect on the net power density as it can be seen in Figure 9B, where a negative power output is reported on day 7th. OCV was also found invariant (1.60±0.03V) with time (Figure 9C) as in the previous cases: this ensures that the procedure adopted (i.e. periodic ED pulses in conjunction with the application of chemical backwashings) does not alter the membrane selectivity features, as expected.

Summarizing, the ED-pulses strategy employed in this long-run was found to be effective in reducing membrane fouling, while a poor effect was observed on the channel clogging issues. This result is of great importance since the physical obstruction of feed spacers should be more reversible than membrane fouling, and, thus, easier to manage. For example, RED stacks equipped with profiled membranes are expected to be less sensitive to clogging issues because of a larger open area (Gurreri et al., 2015). Notably, in some cases profiled membranes were even proven to be more effective than spacers in improving net power output (La Cerva et al., 2017). Furthermore, clogging issues while feeding a RED unit with real seawater and river water have been recently tackled in literature by using periodic air and/or CO_2 injections (Moreno et al., 2017; David A. Vermaas et al., 2014a). These procedures should also be taken into account in the future as complementary strategies to yield a fast and more effective recovery from pressure drops increase in RED operation with wastewaters.

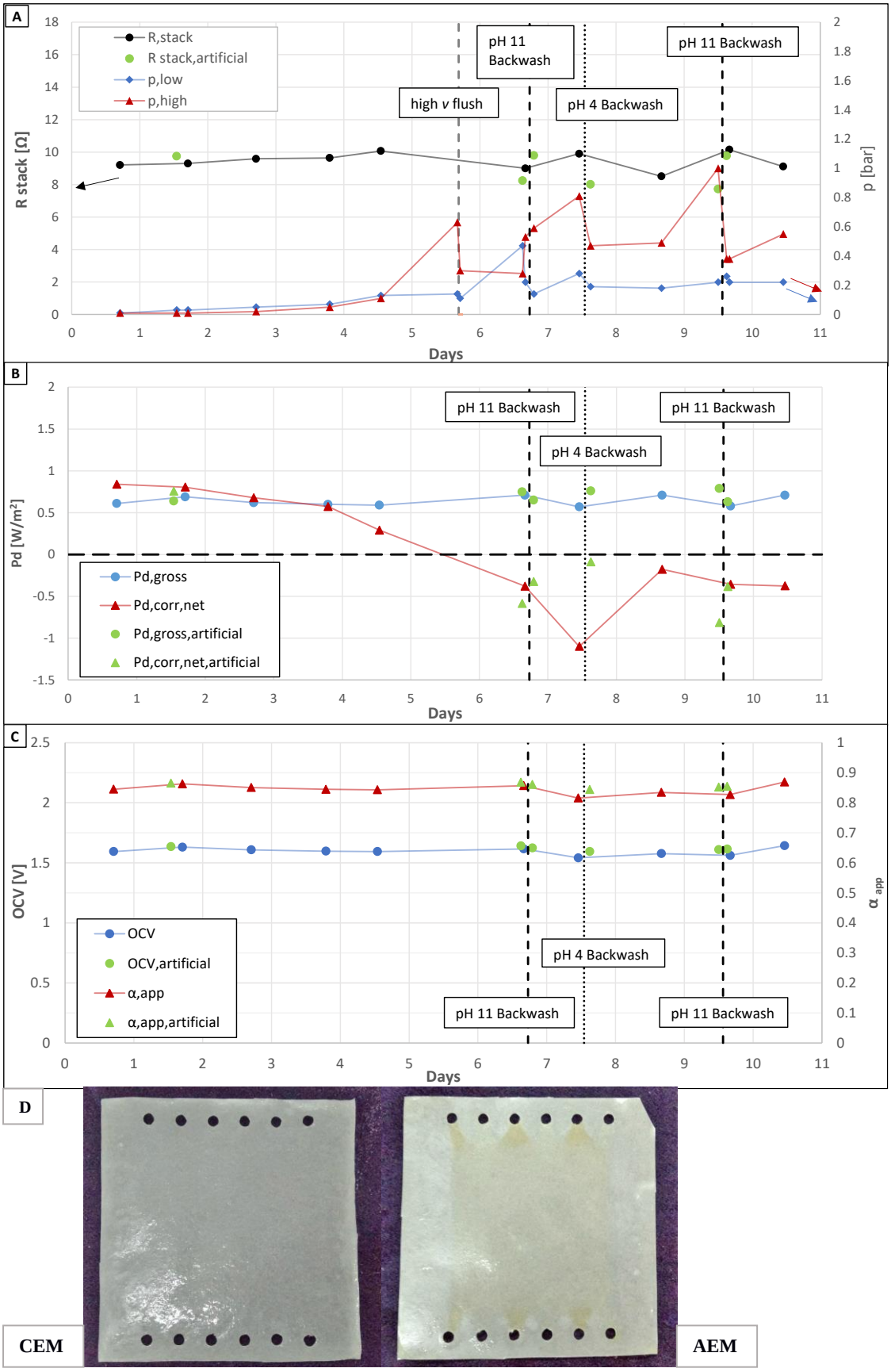

Figure 9. Time evolution of selected parameters for long-run IV (Periodic ElectroDialysis-Pulses), showing: (A) Pressure drops for the high and low compartments and R_{stack}; (B) Gross and corrected net power density; (C) Open circuit voltage and apparent perm-selectivity; and (D) Picture of ion exchange membranes after the long-run. Spot test with artificial solutions are shown in green (●), backwashings are indicated with vertical lines.

4.2 Long-Run V: Fish wastewater (Λ=87.5 mS/cm) / Reclaimed water

In this long-run, small changes were adopted in order to improve the system performance:

- Mild acidification of reclaimed water to reach a final pH = 4 before being used as feed.
- Change v_{low} from 1.0 cm/s to 0.5 cm/s.

Moreover, the concentration of the fish wastewater was higher due to a variation in the outlet stream of the AGS pilot plant, as reported in Table 1. Notably, no effect was found in the biologic treatment step as the AGS-SBALR can withstand up to 75 g/l NaCl without a considerable efficiency loss (Capodici et al., 2018; Corsino et al., 2016).

The first change was mild acidification of the reclaimed water samples to prevent bacteria growth inside the RED unit. The long-run I (section 3.2) showed that during recirculating feed mode the pH of fish wastewater rises above 4, and thus bacteria can grow over the membranes leading to biofouling. Note that this necessity arises from preventing potential biofouling due to the fish wastewater, not due to the reclaimed water. The second change consisted in lowering the fluid velocity of reclaimed water feed from 1.0 cm/s to 0.5 cm/s in order to reduce the pressure drops, whose effect on system performance is expected to be higher than the non-ohmic resistance increase.

The presence of fouling was not evident at simple sight as suggested by the clearer appearance of IEMs after the long-run (Figure 10D). However, the slightly increasing R_{stack} trend (and the corresponding slightly decreasing $P_{d,gross}$ trend) reveals the development of fouling, although produced at lower extent during longer operation time in comparison with the previous long-runs (Figure 10A and 12B). This suggests a positive effect of the initial mild acidification adopted. Moreover, a beneficial effect could be derived by the simultaneous adoption of the ED-pulses procedure, which was not adopted in this long-run. Note that the lower mean value of R_{stack} compared to the previous long-runs is due to the higher conductivity of the reclaimed water (see Table 1).

Regarding the chemical backwashings, a hypochlorite backwashing was tested to further prevent biofouling, as it could be a complementary, economic and environmentally friendly option. Also in this case, the chemical cleaning effect on the membranes material was not detrimental, as indicated by the constant trend of the OCV (Figure 10C) and by the aspect of the IEMs after the long-run (Figure 10D). Some of the potential foulants that were purged during these cleaning procedures were accumulated at the outlet of the RED unit: inspection of the unmounted RED unit showed a sort of agglomerated paste around the edges of the outlets (Figure 10D). However, this material was practically absent in the spacers mesh and also absent over the membranes surfaces, which indicates the effectiveness of the cleaning techniques. Chemical and physical backwashings along with the small changes adopted in this long-run were effective in lowering pressure drops,

which were kept at low values during the course of the long-run and never exceeded 0.5 bar (Figure 10A). More important, despite the slightly decreasing trend, positive values of $P_{d,net,corr}$ were obtained for the full duration of the long-run (29 days) and without reporting any negative value (Figure 10B).

The higher concentration of the fish wastewater provided a poor OCV enhancement (due to the simultaneous higher concentration of the reclaimed water), while a significant permselectivity reduction was found (Figure 10C): in particular, α_{app} decreases from about 90% (other long-runs) to about 75% due to an increase of co-ion concentration inside the membranes (in both CEM and AEM) (Kamcev et al., 2015).

CONCLUSIONS

To the authors' knowledge, this study presents for the first time in literature the analysis of the time evolution performance of a RED unit fed with real wastewaters during long-run experiments. Five long-runs were carried out uninterruptedly for at least ten days, a period likely compatible with the maintenance frequency in larger scale plants. Wastewaters originate from a biological treatment of a high salinity waste stream produced by a fish canning factory (concentrated stream), and of a civil wastewater treated with a Membrane BioReactor (diluted stream). Soft pre-treatments (i.e. soft filtration and mild acidification) were needed before feeding the fish water to the RED unit, while a mild acidification (long-run V) and storage in opaque tanks were sufficient for the reclaimed water.

The results of the long-runs showed that it is possible (i) to produce energy from these treated wastewaters and (ii) to obtain values comparable to those reported in literature for the case of clean artificial solutions of similar salinity. On the other hand, it is also shown that a positive net power over time can be produced only if a proper fouling management is adopted, since channels clogging and membrane fouling dramatically affect the system performance. The visual observation of the membranes after the long-runs along with the data collected analysis was useful to gain indirect information on membrane fouling features. In particular, anion exchange membranes were more sensitive to bio- and organic fouling as observed in their dark brown dyeing after the long-runs, while no perceptible changes were observed in CEMs.

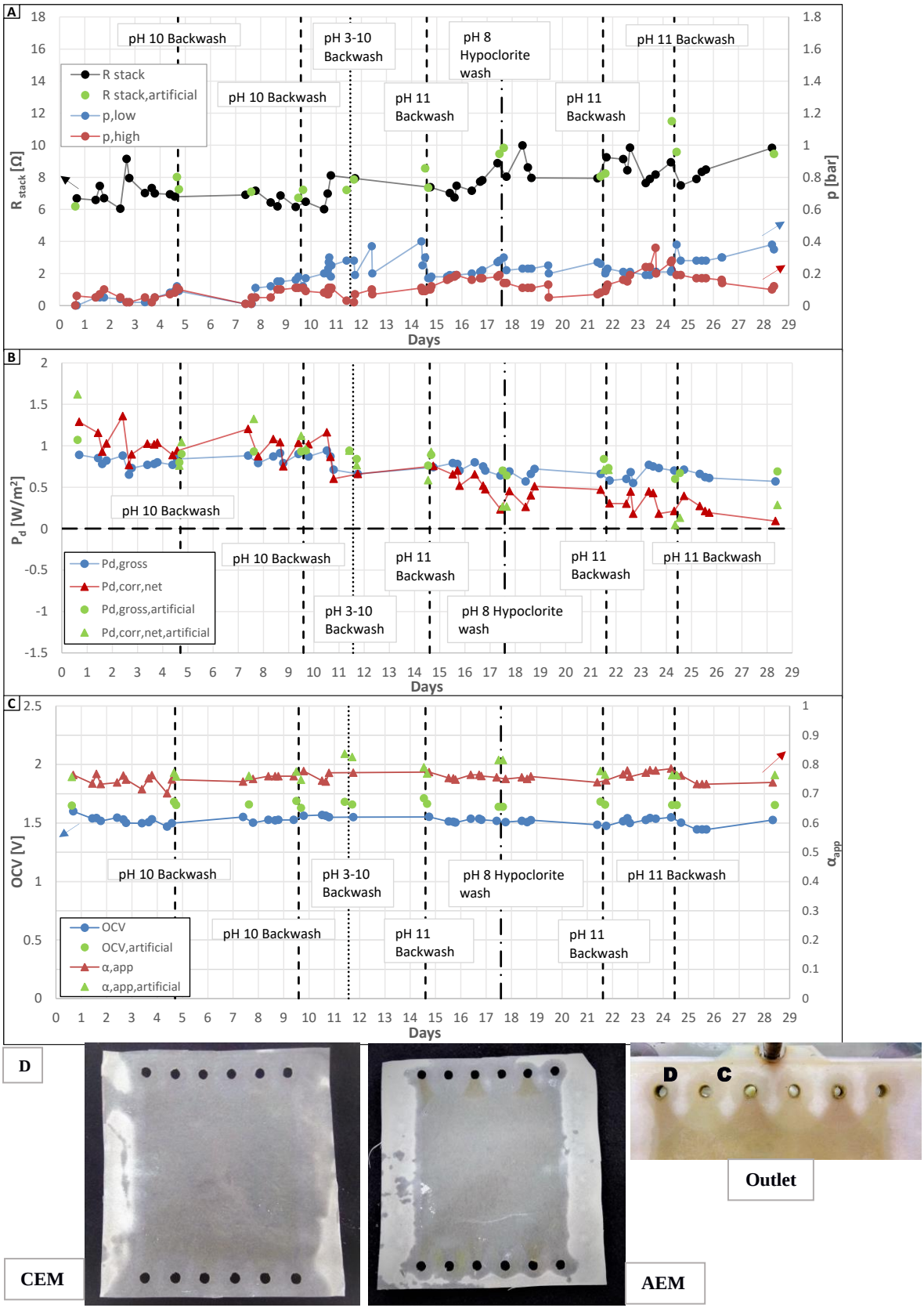

Figure 10. Time evolution of selected parameters for long-run V, showing: (A) Pressure drops for the high and low compartments and R_{stack}; (B) Gross and corrected net power density; (C) Open circuit voltage and apparent perm-selectivity; and (D) Pictures of ion exchange membranes after the long-run and of the outlet right after unmounting the RED unit (D=Diluted, C=Concentrated). Spot test with artificial solutions are shown in green (●), backwashings are indicated with vertical lines.

Physical and chemical *in-situ* backwashings were tested as simple methods to reduce fouling issues. The results collected suggest that a daily flushing in the form of short consecutive pulses (1-2 seconds) at very high flow rates (about 10 cm/s) is an essential practice to prevent an excessive accumulation of matter inside the RED unit channels, particularly when the wastewater has high levels of organic load and when meshed feed spacers are used. Even, the use of chemical backwashings cannot be avoided to keep pressure loss at reasonable values. In particular, the alkaline backwashing was found more efficient for the fouling produced by the fish wastewater, while distilled water at high flow rate was sufficient to obtain similar recovery for the fouling produced by the reclaimed water. On the other hand, the side-effects of these chemical treatments on the system should be studied in more detail. No effect was found on membrane perm-selectivity, while some changes were recorded in R_{stack}. More precisely, in some cases R_{stack} decreased after an alkaline treatment, in other cases it was found to increase. This evidence maybe due to a different membrane behavior depending on (i) the specific condition (in terms of fouling) of the membrane and (ii) the local (i.e. near the membrane) wastewaters features, just before the chemical treatment. These hypotheses are somehow confirmed by a separate experiment (not shown for brevity) with artificial (NaCl-water) solutions only where no effect of alkaline (pH=11) and acid (pH=3) backwashings on membrane performance was observed. However, additional specific studies are needed to fully evaluate the effect.

However, the adoption of these backwashings was not sufficient to guarantee a stable power production of the RED unit over time. In order to improve system performance, additional anti-fouling strategies were tested. The use of periodic ED-pulses was found to prevent foulants adsorption over the membrane surface thus guaranteeing a somehow constancy of R_{stack} over time. Similarly, a mild acidification of the reclaimed water along with a decreased flow rate were able to keep pressure drops at values so low that only positive net power density values were obtained. These strategies were singularly tested and were not able to fully tackle the fouling issue thus leaving room for further investigations. For instance, the simultaneous adoption of both the above strategies could result in a stable operation of the system. In addition, the use of profiled membranes and the adoption of supplementary/alternative procedures such as the use of air and/or CO2 injection pulses (Moreno et al., 2017) could also be beneficial for the process.

On overall, the present work represents the first attempt in the literature to manage waste solutions in a lab-scale RED unit. Collected findings suggest that it is feasible to produce power from these wastes, although additional research efforts are needed to improve the performance of the process. The use of waste streams as feeds in RED may greatly extend the conventional availability of salinity gradient sources and may open promising scenarios for suitable integrations with wastewater treatment plants, where unworthy streams may positively contribute to process

economy.

NOMENCLATURE

Acronym	Meaning
AEM	Anion Exchange Membrane
CEM	Cation Exchange Membrane
DBL	Double Boundary Layer
ED	Electrodialysis
IEM	Ion Exchange Membrane
RED	Reverse Electrodialysis
Symbol	**Parameter (units)**
A	Active cell-pair area (m^2)
C_{high}	Concentration of high salinity solution (($mol.dm^{-3}$))
C_{low}	Concentration of low salinity solution ($mol.dm^{-3}$)
E_{stack}	RED unit electric potential (V)
I_{stack}	RED unit electric current (A)
N	Number of cell-pairs
OCV_{ideal}	Theoretical Open Circuit Voltage (V)
OCV_{exp}	Measured Open Circuit Voltage (V)
$P_{d,gross}$	Gross power density (W/m^2)
$P_{d,corr}$	Corrected power density (W/m^2)
$P_{d,loss}$	Pumping losses power density (W/m^2)
$P_{d,net}$	Net power density (W/m^2)
$P_{d,corr,net}$	Corrected net power density (W/m^2)
p_{high}	Pressure drops in the high channel (bar)
p_{low}	Pressure drops in the low channel (bar)
R_{blank}	Blank electrical resistance (Ω)
R_{CEM}	CEM electrical resistance (Ω)
R_{low}	Low salinity compartment electrical resistance (Ω)
R_{high}	High salinity compartment electrical resistance (Ω)
$R_{non-ohmic}$	Non-ohmic electrical resistance (Ω)
R_{stack}	RED unit electrical resistance (Ω)
v_{high}	Fluid velocity of high feed solution ($cm.s^{-1}$)
v_{low}	Fluid velocity of low feed solution ($cm.s^{-1}$)
Greek Symbol	
α_{app}	IEMs apparent perm-selectivity
γ_{high}	NaCl activity coefficient of the high salinity feed
γ_{low}	NaCl activity coefficient of the low salinity feed
Λ	Electrical conductivity ($mS.cm^{-1}$)
τ	Response time when switching from RED to ED operation (s)

Acknowledgements

This work has been carried out within the REvivED project (www.revivedwater.eu), financed by the European Union's Horizon 2020 research and innovation program under grant agreement N° 685579.

The authors are grateful to their colleagues Prof. Michele Torregrossa, Prof. Giorgio Mannina, Prof. Gaspare Viviani, Dr. Marco Capodici and Dr. Fabio Corsino, from the Department of Civil, Environmental and Materials Engineering (DICAM) of the University of Palermo, for providing the treated effluents used for the experimental campaign and for their advices, useful for optimizing the experimental procedure implemented in this work.

REFERENCES

Alvarez-Silva, O.A., Osorio, A.F., Winter, C., 2016. Practical global salinity gradient energy potential. Renew. Sustain. Energy Rev. 60, 1387–1395. https://doi.org/10.1016/j.rser.2016.03.021

Avci, A.H., Sarkar, P., Tufa, R.A., Messana, D., Argurio, P., Fontananova, E., Di Profio, G., Curcio, E., 2016. Effect of Mg 2+ ions on energy generation by Reverse Electrodialysis. J. Memb. Sci. 520, 499–506. https://doi.org/10.1016/j.memsci.2016.08.007

Badessa, T., Shaposhnik, V., 2016. The electrodialysis of electrolyte solutions of multi-charged cations. J. Memb. Sci. 498, 86–93. https://doi.org/10.1016/j.memsci.2015.09.017

Badessa, T., Shaposhnik, V., 2014. The dependence of electrical conductivity of Ion-Exchange Membranes on the charge of counter ion ©. КОНДЕНСИРОВАННЫЕ СРЕДЫ И МЕЖФАЗНЫЕ ГРАНИЦЫ (In English) 16, 129–133.

Bevacqua, M., Carubia, A., Cipollina, A., Tamburini, A., Tedesco, M., Micale, G., 2016. Performance of a RED system with Ammonium Hydrogen Carbonate solutions. Desalin. Water Treat. 57, 23007–23018. https://doi.org/10.1080/19443994.2015.1126410

Bevacqua, M., Tamburini, A., Papapetrou, M., Cipollina, A., Micale, G., Piacentino, A., 2017. Reverse electrodialysis with NH4HCO3-water systems for heat-to-power conversion. Energy 137, 1293–1307. https://doi.org/10.1016/j.energy.2017.07.012

Cambridge, M.L., Zavala-Perez, A., Cawthray, G.R., Mondon, J., Kendrick, G.A., 2017. Effects of high salinity from desalination brine on growth, photosynthesis, water relations and osmolyte concentrations of seagrass Posidonia australis. Mar. Pollut. Bull. 115, 252–260. https://doi.org/10.1016/j.marpolbul.2016.11.066

Capodici, M., Corsino, S.F., Torregrossa, M., Viviani, G., 2018. Shortcut nitrification-denitrification by means of autochthonous halophilic biomass in an SBR treating fish-canning wastewater. J. Environ. Manage. 208, 142–148. https://doi.org/10.1016/j.jenvman.2017.11.055

Corsino, S.F., Capodici, M., Morici, C., Torregrossa, M., Viviani, G., 2016. Simultaneous nitritation-denitritation for the treatment of high-strength nitrogen in hypersaline wastewater by aerobic granular sludge. Water Res. https://doi.org/10.1016/j.watres.2015.10.041

Cosenza, A., Di Bella, G., Mannina, G., Torregrossa, G., Viviani, G., 2013. Biological Nutrient Removal and Fouling Phenomena in a University of Cape Town Membrane Bioreactor Treating High Nitrogen Loads. J. Environ. Eng. 139, 773–780. https://doi.org/10.1061/(ASCE)EE.1943-7870

D'Angelo, A., Tedesco, M., Cipollina, A., Galia, A., Micale, G., Scialdone, O., 2017. Reverse electrodialysis performed at pilot plant scale: Evaluation of redox processes and simultaneous generation of electric energy and treatment of wastewater. Water Res. 125, 123–131. https://doi.org/10.1016/j.watres.2017.08.008

Daniilidis, A., Herber, R., Vermaas, D.A., 2014a. Upscale potential and financial feasibility of a reverse electrodialysis power plant. Appl. Energy. https://doi.org/10.1016/j.apenergy.2013.12.066

Daniilidis, A., Vermaas, D.A., Herber, R., Nijmeijer, K., 2014b. Experimentally obtainable energy from mixing river water, seawater or brines with reverse electrodialysis. Renew. Energy. https://doi.org/10.1016/j.renene.2013.11.001

Emdadi, A., Gikas, P., Farazaki, M., Emami, Y., 2016. Salinity gradient energy potential at the hyper saline Urmia Lake - ZarrinehRud River system in Iran. Renew. Energy 86, 154–162. https://doi.org/10.1016/j.renene.2015.08.015

Galama, A.H., Vermaas, D.A., Veerman, J., Saakes, M., Rijnaarts, H.H.M., Post, J.W., Nijmeijer, K., 2014. Membrane resistance: The effect of salinity gradients over a cation exchange membrane. J. Memb. Sci. https://doi.org/10.1016/j.memsci.2014.05.046

Garcia-Vasquez, W., Dammak, L., Larchet, C., Nikonenko, V., Grande, D., 2016. Effects of acid-base cleaning procedure on structure and properties of anion-exchange membranes used in electrodialysis. J. Memb. Sci. https://doi.org/10.1016/j.memsci.2016.02.006

Güler, E., van Baak, W., Saakes, M., Nijmeijer, K., 2014. Monovalent-ion-selective membranes for reverse electrodialysis. J. Memb. Sci. 455. https://doi.org/10.1016/j.memsci.2013.12.054

Guo, W., Ngo, H.H., Li, J., 2012. A mini-review on membrane fouling. Bioresour. Technol. 122, 27–34. https://doi.org/10.1016/j.biortech.2012.04.089

Gurreri, L., Ciofalo, M., Cipollina, A., Tamburini, A., Van Baak, W., Micale, G., 2015. CFD modelling of profiled-membrane channels for reverse electrodialysis. Desalin. Water Treat. 55, 3404–3423. https://doi.org/10.1080/19443994.2014.940651

Gurreri, L., Tamburini, A., Cipollina, A., Micale, G., 2012. CFD analysis of the fluid flow behavior in a reverse electrodialysis stack. Desalin. Water Treat. 48, 390–403. https://doi.org/10.1080/19443994.2012.705966

Gurreri, L., Tamburini, A., Cipollina, A., Micale, G., Ciofalo, M., 2016. Flow and mass transfer in spacer-filled channels for reverse electrodialysis: a CFD parametrical study. J. Memb. Sci. 497, 300–317. https://doi.org/10.1016/j.memsci.2015.09.006

Gurreri, L., Tamburini, A., Cipollina, A., Micale, G., Ciofalo, M., 2014. CFD prediction of concentration polarization phenomena in spacer-filled channels for reverse electrodialysis. J. Memb. Sci. 468, 133–148.

https://doi.org/10.1016/j.memsci.2014.05.058
Helfer, F., Lemckert, C., 2015. The power of salinity gradients: An Australian example. Renew. Sustain. Energy Rev. 50, 1–16. https://doi.org/10.1016/j.rser.2015.04.188
Helfer, F., Lemckert, C., Anissimov, Y.G., 2014. Osmotic power with Pressure Retarded Osmosis: Theory, performance and trends - A review. J. Memb. Sci. 453, 337–358. https://doi.org/10.1016/j.memsci.2013.10.053
Hirani, Z.M., Bukhari, Z., Oppenheimer, J., Jjemba, P., LeChevallier, M.W., Jacangelo, J.G., 2013. Characterization of effluent water qualities from satellite membrane bioreactor facilities. Water Res. 47, 5065–5075. https://doi.org/10.1016/j.watres.2013.05.048
Hong, J.G., Zhang, B., Glabman, S., Uzal, N., Dou, X., Zhang, H., Wei, X., Chen, Y., 2015. Potential ion exchange membranes and system performance in reverse electrodialysis for power generation: A review. J. Memb. Sci. https://doi.org/10.1016/j.memsci.2015.02.039
Jia, Z., Wang, B., Song, S., Fan, Y., 2014. Blue energy: Current technologies for sustainable power generation from water salinity gradient. Renew. Sustain. Energy Rev. 31, 91–100. https://doi.org/10.1016/j.rser.2013.11.049
Kamcev, J., Paul, D.R., Manning, G.S., Freeman, B.D., 2015. Ion activity coefficients in ion exchange polymers: Applicability of Manning's counterion condensation theory. ACS Appl. Mater. Interfaces 48, 8011–8024. https://doi.org/10.1021/acs.macromol.5b01654
Katz, W.E., 1979. THE ELECTRODIALYSLS REVERSAL (EDR) PROCESS A brief description , history of development and operating data on first experience with the electrodialysis reversal process are given . EDR consti- tutes an improvement on the ED process by providing automati 28, 31–40.
Kingsbury, R.S., Liu, F., Zhu, S., Boggs, C., Armstrong, M.D., Call, D.F., Coronell, O., 2017. Impact of natural organic matter and inorganic solutes on energy recovery from five real salinity gradients using reverse electrodialysis. J. Memb. Sci. 541, 621–632. https://doi.org/10.1016/j.memsci.2017.07.038
La Cerva, M.L., Liberto, M. Di, Gurreri, L., Tamburini, A., Cipollina, A., Micale, G., Ciofalo, M., 2017. Coupling CFD with a one-dimensional model to predict the performance of reverse electrodialysis stacks. J. Memb. Sci. 541, 595–610. https://doi.org/10.1016/j.memsci.2017.07.030
La Mantia, F., Pasta, M., Deshazer, H.D., Logan, B.E., Cui, Y., 2011. Water salinity difference. Nano 11, 1810–1813. https://doi.org/10.1021/nl200500s
Lee, H.-J., Moon, S.-H., Tsai, S.-P., 2002. Effects of pulsed electric fields on membrane fouling in electrodialysis of NaCl solution containing humate. Sep. Purif. Technol. 27, 89–95. https://doi.org/10.1016/S1383-5866(01)00167-8
Lee, H., Hong, M., Han, S., Cho, S., 2009. Fouling of an anion exchange membrane in the electrodialysis 238, 60–69.
Lee, H.J., Kim, D.H., Cho, J., Moon, S.H., 2003. Characterization of anion exchange membranes with natural organic matter (NOM) during electrodialysis. Desalination 151, 43–52. https://doi.org/10.1016/S0011-9164(02)00971-2
Lee, H.J., Moon, S.H., 2005. Enhancement of electrodialysis performances using pulsing electric fields during extended period operation. J. Colloid Interface Sci. 287, 597–603. https://doi.org/10.1016/j.jcis.2005.02.027
Lee, H.J., Strathmann, H., Moon, S.H., 2006. Determination of the limiting current density in electrodialysis desalination as an empirical function of linear velocity. Desalination 190, 43–50. https://doi.org/10.1016/j.desal.2005.08.004
Lefebvre, O., Moletta, R., 2006. Treatment of organic pollution in industrial saline wastewater: A literature review. Water Res. https://doi.org/10.1016/j.watres.2006.08.027
Mikhaylin, S., Bazinet, L., 2016. Fouling on ion-exchange membranes: Classification, characterization and strategies of prevention and control. Adv. Colloid Interface Sci. 229, 34–56. https://doi.org/10.1016/j.cis.2015.12.006
Moreno, J., de Hart, N., Saakes, M., Nijmeijer, K., 2017. CO2 saturated water as two-phase flow for fouling control in reverse electrodialysis. Water Res. 125, 23–31. https://doi.org/10.1016/j.watres.2017.08.015
Pawlowski, S., Crespo, J.G., Velizarov, S., 2014a. Pressure drop in reverse electrodialysis: Experimental and modeling studies for stacks with variable number of cell pairs. J. Memb. Sci. https://doi.org/10.1016/j.memsci.2014.03.020
Pawlowski, S., Galinha, C.F., Crespo, J.G., Velizarov, S., 2016. 2D fluorescence spectroscopy for monitoring ion-exchange membrane based technologies - Reverse electrodialysis (RED). Water Res. 88, 184–198. https://doi.org/10.1016/j.watres.2015.10.010
Pawlowski, S., Sistat, P., Crespo, J.G., Velizarov, S., 2014b. Mass transfer in reverse electrodialysis: Flow entrance effects and diffusion boundary layer thickness. J. Memb. Sci. 471, 72–83. https://doi.org/10.1016/j.memsci.2014.07.075
Raffin, M., Germain, E., Judd, S., 2013. Wastewater polishing using membrane technology: A review of existing installations. Environ. Technol. (United Kingdom) 34, 617–627. https://doi.org/10.1080/09593330.2012.710385
Rica, R., Ziano, R., Salerno, D., Mantegazza, F., van Roij, R., Brogioli, D., 2013. Capacitive Mixing for Harvesting the Free Energy of Solutions at Different Concentrations. Entropy 15, 1388–1407. https://doi.org/10.3390/e15041388
Roberts, D.A., Johnston, E.L., Knott, N.A., 2010. Impacts of desalination plant discharges on the marine environment: A critical review of published studies. Water Res. 44, 5117–5128. https://doi.org/10.1016/j.watres.2010.04.036
Rubinstein, I., Zaltzman, B., 2000. Electro-osmotically induced convection at a permselective membrane. Phys. Rev. E - Stat. Physics, Plasmas, Fluids, Relat. Interdiscip. Top. 62, 2238–2251. https://doi.org/10.1103/PhysRevE.62.2238
Ruiz, B., Sistat, P., Huguet, P., Pourcelly, G., Araya-Farias, M., Bazinet, L., 2007. Application of relaxation periods during electrodialysis of a casein solution: Impact on anion-exchange membrane fouling. J. Memb. Sci. 287, 41–

50. https://doi.org/10.1016/j.memsci.2006.09.046
Sarp, S., Li, Z., Saththasivam, J., 2016. Pressure Retarded Osmosis (PRO): Past experiences, current developments, and future prospects. Desalination 389, 2–14. https://doi.org/10.1016/j.desal.2015.12.008
Schaetzle, O., Buisman, C.J.N., 2015. Salinity Gradient Energy: Current State and New Trends. www.engineering.org.cn News Focus Eng. 1, 164–166. https://doi.org/10.15302/J-ENG-2015046
Scialdone, O., Albanese, A., D'Angelo, A., Galia, A., Guarisco, C., 2013. Investigation of electrode material - Redox couple systems for reverse electrodialysis processes. Part II: Experiments in a stack with 10-50 cell pairs. J. Electroanal. Chem. https://doi.org/10.1016/j.jelechem.2013.06.001
Sivaprakasam, S., Mahadevan, S., Sekar, S., Rajakumar, S., 2008. Biological treatment of tannery wastewater by using salt-tolerant bacterial strains. Microb. Cell Fact. 7, 1–7. https://doi.org/10.1186/1475-2859-7-15
Straub, A.P., Deshmukh, A., Elimelech, M., 2016. Pressure-retarded osmosis for power generation from salinity gradients: is it viable? Energy Environ. Sci. 9, 31–48. https://doi.org/10.1039/C5EE02985F
Tanaka, Y., 2005. Limiting current density of an ion-exchange membrane and of an electrodialyzer. J. Memb. Sci. 266, 6–17. https://doi.org/10.1016/j.memsci.2005.05.005
Tedesco, M., Brauns, E., Cipollina, A., Micale, G., Modica, P., Russo, G., Helsen, J., 2015. Reverse electrodialysis with saline waters and concentrated brines: A laboratory investigation towards technology scale-up. J. Memb. Sci. https://doi.org/10.1016/j.memsci.2015.05.020
Tedesco, M., Cipollina, A., Tamburini, A., Micale, G., 2017. Towards 1 kW power production in a reverse electrodialysis pilot plant with saline waters and concentrated brines. J. Memb. Sci. 522, 226–236. https://doi.org/10.1016/j.memsci.2016.09.015
Tedesco, M., Mazzola, P., Tamburini, A., Micale, G., Bogle, I.D.L., Papapetrou, M., Cipollina, A., 2015. Analysis and simulation of scale-up potentials in reverse electrodialysis. Desalin. Water Treat. 55, 3391–3403. https://doi.org/10.1080/19443994.2014.947781
Tedesco, M., Scalici, C., Vaccari, D., Cipollina, A., Tamburini, A., Micale, G., 2016. Performance of the first reverse electrodialysis pilot plant for power production from saline waters and concentrated brines. J. Memb. Sci. 500, 33–45. https://doi.org/10.1016/j.memsci.2015.10.057
Vanoppen, M., Bakelants, A.F.A.M., Gaublomme, D., Schoutteten, K.V.K.M., Van Den Bussche, J., Vanhaecke, L., Verliefde, A.R.D., 2015. Properties governing the transport of trace organic contaminants through ion-exchange membranes. Environ. Sci. Technol. 49, 489–497. https://doi.org/10.1021/es504389q
Vaselbehagh, M., Karkhanechi, H., Takagi, R., Matsuyama, H., 2017. Biofouling phenomena on anion exchange membranes under the reverse electrodialysis process. J. Memb. Sci. 530, 232–239. https://doi.org/10.1016/j.memsci.2017.02.036
Veerman, J., Saakes, M., Metz, S.J., Harmsen, G.J., 2010. Electrical power from sea and river water by reverse electrodialysis: A first step from the laboratory to a real power plant. Environ. Sci. Technol. https://doi.org/10.1021/es1009345
Veerman, J., Saakes, M., Metz, S.J., Harmsen, G.J., 2009. Reverse electrodialysis: Performance of a stack with 50 cells on the mixing of sea and river water. J. Memb. Sci. https://doi.org/10.1016/j.memsci.2008.11.015
Vermaas, D.A., Kunteng, D., Saakes, M., Nijmeijer, K., 2013. Fouling in reverse electrodialysis under natural conditions. Water Res. https://doi.org/10.1016/j.watres.2012.11.053
Vermaas, D.A., Kunteng, D., Veerman, J., Saakes, M., Nijmeijer, K., 2014a. Periodic feed water reversal and air sparging as anti fouling strategies in reverse electrodialysis: Supporting Information. Water Res. 48, 1–6.
Vermaas, D.A., Saakes, M., Nijmeijer, K., 2014b. Early detection of preferential channeling in reverse electrodialysis. Electrochim. Acta 117, 9–17. https://doi.org/10.1016/j.electacta.2013.11.094
Vermaas, D.A., Veerman, J., Saakes, M., Nijmeijer, K., 2014c. Influence of multivalent ions on renewable energy generation in reverse electrodialysis. Energy Environ. Sci. 7, 1434–1445. https://doi.org/10.1039/C3EE43501F
Wang, Q., Gao, X., Zhang, Y., He, Z., Ji, Z., Wang, X., Gao, C., 2017. Hybrid RED/ED system: Simultaneous osmotic energy recovery and desalination of high-salinity wastewater. Desalination. https://doi.org/10.1016/j.desal.2016.12.005
Wang, Z., Gao, M., She, Z., Wang, S., Jin, C., Zhao, Y., Yang, S., Guo, L., 2015. Effects of salinity on performance, extracellular polymeric substances and microbial community of an aerobic granular sequencing batch reactor. Sep. Purif. Technol. 144, 223–231. https://doi.org/10.1016/j.seppur.2015.02.042
Xiao, Y., Roberts, D.J., 2010. A review of anaerobic treatment of saline wastewater. Environ. Technol. 31, 1025–1043. https://doi.org/10.1080/09593331003734202
Yip, N.Y., Vermaas, D.A., Nijmeijer, K., Elimelech, M., 2014. Thermodynamic, energy efficiency, and power density analysis of reverse electrodialysis power generation with natural salinity gradients. Environ. Sci. Technol. https://doi.org/10.1021/es5005413

SUPPLEMENTARY INFORMATION

S1. Data processing and monitoring

Electrical parameters were measured under Open Circuit Voltage (OCV) conditions, and closing the circuit with an external load with variable resistance.

The OCV experimentally measured, can be calculated by the Nernst equation considering NaCl only as follows:

$$OCV_{exp} = \alpha \cdot 2N \frac{RT}{z_i F} \cdot ln\left(\frac{\gamma_{high} \cdot C_{high}}{\gamma_{low} \cdot C_{low}}\right) \quad (1)$$

Where α is the average perm-selectivity coefficient of the membranes, R= 8.314 J·mol^{-1}·K^{-1} is the gas constant, F= 96485 C·mol^{-1} is Faraday constant, T is temperature, z_i the charge of ion i, N is the number of cell pairs and γ_{high}, C_{high}, γ_{low}, C_{low} the activity coefficients (Haynes, 2012) and concentrations of the concentrate and dilute solutions, respectively. The ideal OCV (OCV_{ideal}) can be derived from this expression assuming $\alpha=1$, i.e. considering ideal membranes.

The ratio between the experimental OCV (OCV_{exp}) and the ideal OCV gives the apparent perm-selectivity coefficient as an average for both ion exchange membranes:

$$\alpha_{app} = \frac{OCV_{exp}}{OCV_{ideal}} \quad (2)$$

OCV_{ideal} for real wastewaters was calculated considering NaCl only, by determining the apparent NaCl concentration from the electrical conductivity of the real samples, thus neglecting the contribution of other ions. This approximation was used given the variations of the composition of the real wastewater samples that were daily collected, and it was satisfactory based on the similar values of α_{app} obtained regardless the use of pure NaCl solution or real wastewaters.

When an external load (R_{ext}) is connected with the electrode connections of the RED unit, a current pass through the circuit and a potential drop occurs due the internal resistance of the stack, as indicated by equation 3:

$$E_{stack} = OCV_{exp} - R_{stack} \cdot I_{stack} \quad (3)$$

Measuring the stack potential (E_{stack}) and the stack current (I_{stack}) while varying the external load, the plot of E_{stack} vs I_{stack} gives a linear relation. The absolute value of the slope represents the internal stack resistance (R_{stack}), while the intercept with the y-axis represents the measured OCV_{exp}. A graphical representation of the E_{stack} vs I_{stack} line is reported in Figure S1A.

Stack resistance can be further split into different contributions, as follows:

$$R_{stack} = N \cdot R_{cell-pair} + R_{non-ohmic} + R_{blank} = N \cdot \left[R_{CEM} + R_{low} + R_{AEM} + R_{high}\right] + R_{non-ohmic} + R_{blank} \quad (4)$$

where R_{AEM}, R_{CEM} are the cation and anion exchange membranes resistances, respectively, R_{low} and R_{high} are the electric resistances of feed compartments, $R_{non\text{-}ohmic}$ is the non-ohmic resistance contribution accounting for cross-stream (polarization) and streamwise solution concentration variation, and R_{blank} accounts for the ERS compartments resistance.

Power produced is also derived from the Ohm's law, and normalizing over the total active membrane area ($N{\cdot}A$) gives the gross power density ($P_{d,\,gross}$) in W/m^2:

$$P_{d,gross} = \frac{E_{stack}^2}{R_{ext}{\cdot}N{\cdot}A} \tag{5}$$

Figure S1B shows the variation of power density output as a function of the measured stack potential. The maximum value of power density is clearly identified as the maximum of the parabola, corresponding to the power generated when the external load is equal to the internal stack resistance, and E_{stack} equals to OCV/2.

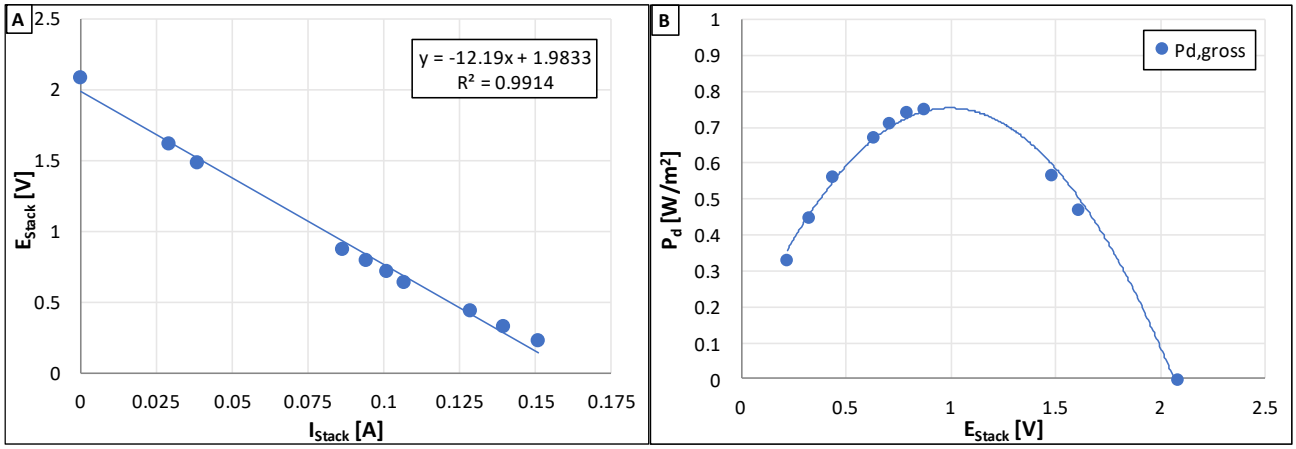

Figure S1. Electrical responses of the RED unit operated with variable external resistances, using artificial NaCl solutions as feeds: C_{low} = 0.004 M, C_{high} = 0.500 M, v_{low} = 1.0 cm/s, v_{high} = 0.5 cm/s. (**A**) Polarization curve, (**B**) (gross) power density vs E_{stack}.

S2. Evaluation of blank resistance and corrected net power density.

When considering extrapolation of the operating performance of a lab-scale RED unit to a larger stack piled with much larger number of cell pairs, the influence of "blank resistance", i.e. of the ohmic and non-ohmic resistances generated in the electrode compartments and end-membranes (CEM) typically becomes negligible. Thus, power density values measured in small laboratory stacks are typically "corrected" in order to account for the effect of blank resistance, in particular, calculating the power potentially generable if the R_{blank} were null.

A typical procedure for such correction is based on the subtraction of R_{blank} from the stack resistance and the re-calculation of new values of E_{stack} and I_{stack} in maximum power output conditions. Thus, rearranging *Eq. 3* and *Eq. 5* gives the so called "corrected power density" (Bevacqua, et al., 2016), $P_{d,gross,corr}$:

$$P_{d,gross,corr} = \frac{OCV^2}{N \cdot A \cdot R_{ext} \cdot \left(1 + \frac{R_{stack} - R_{blank}}{R_{ext}}\right)^2} \quad (6)$$

The blank resistance was experimentally determined by measuring R_{stack} for RED units piled with different number of cell pairs and performing a linear regression of R_{stack} with the cell pairs number: the intercept at $N=0$ gives R_{blank}. Figure S2A shows the R_{blank} determination for the RED unit used in long-run I, which was found the same also for long-runs II and III (3.65 Ω). For the long-runs IV and V the R_{blank} was found equal to 2.00 Ω (not shown).

Finally, the power density required for pumping the solutions ($P_{d,loss}$) to the RED unit can be estimated by the following expression:

$$P_{d,loss} = \frac{\Delta p_{high} \cdot Q_{high} + \Delta p_{low} \cdot Q_{low}}{N \cdot A} \quad (7)$$

where Δp indicates the pressure drop in the *high* or *low* concentration compartment and Q the relevant flow rate. By subtracting the pumping losses to the corrected power density, the corrected net power density, $P_{d,net,corr}$ is obtained:

$$P_{d,net,corr} = P_{d,gross,corr} - P_{d,loss} \quad (8)$$

Corrections of the gross power density (blank resistance subtraction and estimation of pumping losses) of a standard case are shown in Figure S2B.

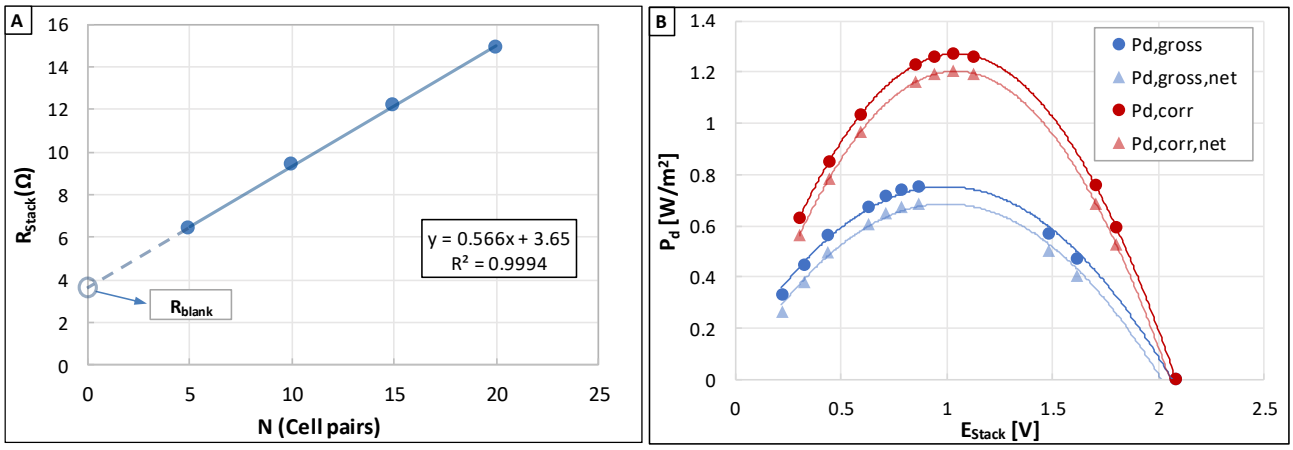

Figure S2. (**A**) Experimental determination of R_{blank} by measuring R_{stack} at different number of cell pairs (N). (**B**) Power density curves obtained with artificial NaCl solutions, C_{low}=0.004 mol/L, C_{high} =0.500 mol/L; v_{low}=1.0 cm/s, v_{high}=0.5 cm/s; 10 cell pairs RED unit. Pressure drops were 0.009 bar (low) and 0.005 bar (high).

References

Bevacqua, M., Carubia, A., Cipollina, A., Tamburini, A., Tedesco, M., Micale, G., 2016. Performance of a RED system with Ammonium Hydrogen Carbonate solutions. Desalin. Water Treat. 57, 23007–23018. https://doi.org/10.1080/19443994.2015.1126410

Haynes, W.M., 2011. CRC Handbook of Chemistry and Physics. 92nd ed. CRC Press: Boca Raton, FL, p 5-108.